ANKARA YILDIRIM BEYAZIT UNIVERSITY

GRADUATE SCHOOL OF NATURAL AND APPLIED SCIENCES

COMBINED SERIAL PARALLEL HYBRID FIBER AMPLIFIER WITH HIGH ORDER RAMAN SCATTERING

M.Sc. Thesis by

Ayman Ibrahim ABOUSEDA

Department of Electric and Electronic Engineering

October, 2019

ANKARA

COMBINED SERIAL PARALLEL HYBRID FIBER AMPLIFIER WITH HIGH ORDER RAMAN SCATTERING

A Thesis Submitted to

The Graduate School of Natural and Applied Sciences of

Ankara Yildirım Beyazit University

In Partial Fulfilment of the Requirements for the Degree of Master of Science in Electric and Eelectronics Engineering, Department of Electric and Electronic Engineering

by

Ayman Ibrahim ABOUSEDA

October, 2019

ANKARA

M.Sc. THESIS EXAMINATION RESULT FORM

We have read the thesis entitled **“COMBINED SERIAL PARALLEL HYBRID FIBER AMPLIFIER WITH HIGH ORDER RAMAN SCATTERING”** completed by **AYMAN ABOUSEDA** under the supervision of **ASSIST. PROF. DR. THAMER AL-MASHHADANI** and we certify that in our opinion it is fully adequate, in scope and in quality, as a thesis for the degree of Master of Science.

Assist. Prof. Dr. Thamer AL-MASHHADANI

Supervisor

Prof. Dr. Şerafettin EREL

Jury member

Prof. Dr. Murat YÜCEL

Jury member

Prof. Dr. Ergün ERASLAN

Director

Graduate School of Natural and Applied Sciences

I hereby declare that, in this thesis which has been prepared in accordance with the Thesis Writing Manual of Graduate School of Natural and Applied Sciences,

- All data, information and documents are obtained in the framework of academic and ethical rules,
- All information, documents and assessments are presented in accordance with scientific ethics and morals,
- All the materials that have been utilized are fully cited and referenced,
- No change has been made on the utilized materials,
- All the works presented are original,

And in any contrary case of above statements, I accept to renounce all my legal rights.

Date: 10.10.2019 **Signature: …………..………………...**

Name & Surname: Ayman ABOUSEDA

ACKNOWLEDGMENTS

All praises to almighty ALLAH, the most merciful and compassionate, who enable me to complete this thesis.

First, I would to extend my heartfelt gratitude and appreciation to my family especially my parents, whose support and encouraging words made me sail smoothly through my difficult times and their full support throughout my education.

I would like to thank my thesis advisor Assist. Prof. Dr. Thamer AL-MASHHADANI for his tremendous support and confidence in me during my thesis study. His immense knowledge and precious recommendations constituted the milestones of this study. His guidance assisted me all the time of my research and while writing this thesis.

I am very grateful to my co-supervisor Assist. Prof. Dr. Mudhafar ALI who I have extremely pleased to be working with him. He has provided me comprehensive professional guidance and taught me a great deal about scientific research at large.

Finally, my thanks to all people who contributed this work in any form.

2019, 10 October **Ayman Ibrahim ABOUSEDA**

COMBINED SERIAL PARALLEL HYBRID FIBER AMPLIFIER WITH HIGH ORDER RAMAN SCATTERING

ABSTRACT

A combined serial parallel hybrid fiber amplifier (CSP-HFA) is enhanced using high order Raman scattering. All the result concluded in this paper are simulated via Optisystem 14. The proposed HFA consist of two Raman fiber amplifiers (RFAs) and Erbium doped fiber amplifier (EDFA). RFA1 is pumped by two Raman pump units (RPUs) with different wavelengths of 1410 nm and 1495 nm. While RFA2 is pumped by 1480 nm is pumped by the residual pump power of the second RFA pump unit. The proposed amplifier setup shows broadly gain flatness that covers short band (S-band), conventional band (C-band) and long band (L-band). The overall gain is tested under different input power ratio inserted to the amplifiers branch. With an input power ratio of 0.8:0.2, at small input signal power of -25 dBm the overall gain flatness of 95 nm (1525 nm-1620 nm) and 19 dB as average gain are recorded. For high input signal power of -15 dBm; different input power ratio of 0.4:0.6 are used to achieve wide overall gain of 85 nm (1530 nm- 1615 nm) and 17 dB average gain level.

Keywords: Combined serial parallel hybrid fiber amplifier, flat gain bandwidth, fiber amplifiers, Raman amplifier, wideband hybrid fiber amplifier, Erbium doped fiber amplifier.

YÜKSEK DERECELİ RAMAN SAÇILMASI İLE BİRLEŞTİRİLMİŞ SERİ PARALEL HİBRİD FİBER YÜKSELTEÇ

ÖZ

Birleştirilmiş seri paralel hibrit fiber yükselteçi (CSP-HFA), yüksek dereceli Raman saçılması kullanılarak geliştirilmiştir. Bu raporda açıklanan tüm sonuçlar Optisystem 14 üzerinden simüle edilmiştir. Önerilen HFA, iki Raman fiber yükselteçinden (RFA) ve Erbium katkılı fiber yükselteçten (EDFA) oluşur. RFA1, 1410 nm ve 1495 nm olmak üzere farklı dalga boylarına sahip iki Raman pompa ünitesi (RPU) tarafından pompalanmıştır. RFA2, 1480 nm tarafından pompalanırken, ikinci RFA pompa ünitesinin artık pompa gücü tarafından pompalanır. Önerilen yükselteç düzeneği, kısa bandı (S bandı), geleneksel bandı (C bandı) ve uzun bandı (L bandı) kapsayan düzleşmeyi göstermektedir. Genel düzleştirilmiş kazanç, yükselteç kollarına verilen farklı giriş gücü oranları için test edilmiştir. 0,8: 0,2 giriş gücü oranıyla -25 dBm'lik küçük giriş sinyal gücünde, ortalama kazanç olarak 95 nm (1525 nm-1620 nm) ve 19 dB toplam düzlük elde edilmiştir. -15 dBm'lik yüksek giriş sinyali gücü için; genel toplam 85 nm (1530 nm - 1615 nm) ve 17 dB ortalama kazanç seviyesine ulaşmak için 0.4: 0.6 farklı giriş gücü oranı kullanılmıştır.

Anahtar kelimeler: Birleştirilmiş seri paralel hibrit fiber yükselteçi, düz kazanç bant genişliği, fiber yükselteç, Raman yükselteçi, geniş bantlı hibrit fiber yükselteç, Erbium katkılı fiber yükselteç.

CONTENTS

NOMENCLATURE

Roman Letter Symbols

g	Gain
g_o	Small Signal Gain Coefficient
p	Signal Power
p_s	Signal power
P_P	Pump Power
g_R	Raman Gain Coefficient
w_P	Angular Frequency of the Pump
w_S	Angular Frequency ofthe Signal
L	Fiber Length
P_{SBS}	Stimulated Brillouin scattering threshold
A_{eff}	Effective Area of the Fiber
g_B	Peak Value of the Brillouin Gain
L_{eff}	Effective Length of the Fiber
G_A	On-off Gain
P_0	Input Pump Power at Z=0
P_{sat}	Saturation Power
P_{ASE}	Amplified spontaneous emission power
B_{opt}	Optical Filter Bandwidth
n_{SP}	Spontaneous Scattering Factor
hv_0	Average Photon Energy
Gav	Average Gain
G_{var}	Gain Variation
G_{max}	Maximum Gain
G_{min}	Minimum Gain
NF_{EDFA}	Erbium Doped Fiber Amplifier Noise Figure
SNR	Signal–to–noise ratio
λ	wavelength
ξ	Takes Values Of ±1
α_S	Attenuation Coefficient of the Signal

Acronym

DCF	Dispersion Compensating Fiber
DWDM	Dense Wavelength Division Multiplexing
EDFA	Erbium Doped Fiber Amplifier
EPU	Erbium Pump Unit
HFA	Hybrid Fiber Amplifier
NF	Noise Figure
OPP	Optimum Pump Power
OPW	Optimum Pump Wavelength
OSA	Optical Spectrum Analyzer
S-HFA	Serial Hybrid Fiber Amplifier
P-HFA	Parallel Hybrid Fiber Amplifier
SNR	Signal to Noise Ratio
RFA	Raman Fiber Amplifier
RPU	Raman Pump Unit
SBS	Stimulated Brillouin Scattering
SMF	Single Mode Fiber
SOA	Semiconductor Optical Amplifier
SRS	Stimulated Raman Scattering
TLS	Tunable Laser Source
WDM	Wavelength Division Multiplexing
CSP-HFA	Combined Serial Parallel Hybrid Fiber Amplifier
S-BAND	Short Band
C-BAND	Conventional Band
L-BAND	Long Band
GE	Germanium
FBG	Fiber Bragg Grating
ASE	Amplified Spontaneous Emission
DRA	Distributed Raman Amplifier
MHZ	Megahertz
GHZ	Gigahertz
THZ	Terahertz
FWM	Four Wave Mixing
DSF	Dispersion Shifted Fiber

LIST OF TABLES

LIST OF FIGURES

CHAPTER 1

INTRODUCTION AND LITERATURE REVIEW

1.1 Overview on Hybrid Optical Amplifier

HFAs are an assuring technology for the next generation of multi-terabit DWDM systems. Notably, hybrid Raman or EDFAs are basically manufactured to increase the bandwidth as well as maximize the span length of EDFAs. Designing an optimized HFA is somewhat complex although with considerable a degree of freedom [1]. There are basically two major configurations used when designing hybrid fiber amplifiers; Serial (S)-HFA and Parallel (P)-HFA. For the serial configuration case, the incoming signal is amplified at two levels established on one path, whereby the signal out of the preceding stage is the incoming signal to stage two. For the case of parallel architecture, the input signal is divided into two wavelength bands (C and L), the gain spectrum flatness is essentially controlled by adjusting the input signal ratio [2]. In a bid to ameliorate the long-haul transmission systems performance, there is a need to increase the transmission capacity as well as the repeater spacing [3]. WDM is demonstrating to be a practicable method for enhancing the transmission bandwidth for fiber-optic communications links [4]. With an increased number of channels in WDM systems, there is need for broad-band spectrally flat amplification [5]. It should be noted that wideband and gain-flattened fiber amplifiers are essential for wideband as well as long-distance WDM optical network systems of 1.5 µm. Enhancing technics for flattened-gain-bandwidth of a fiber amplifier use conventional host materials, gain equalizers (GEQ’s) and two-gain-band parallel-configurations for EDFAs [6]. The compensating modules for dispersion for the case of Raman amplification in dispersion-compensating fiber (DCF) are taken to be an appealing means as well as a promising tool for the next generation long-haul optical communication systems of high-capacity, and their system applications have been thoroughly exposited. DCF-based Raman amplifiers can compensate for both dispersion and losses in a given transmission fiber span, and nonetheless a surplus net Raman gain between 10–20 dB may also be achieved easily after background fiber loss compensation due to the fact that DCF possess a nonlinearity that is 7–8 times higher than the standard single-mode fiber (SMF) because of the high germanium (GE) concentration and the small core size. In a DCF-based Raman amplification, one essential issue is to enhance pump power efficiency because of the fact that a considerable quantity of pump power is not used and therefore wasted because of the short length of the DCF. Its worthy to note that the DCF length that is applied in dispersion-compensating modules is ascertained by taking into account the required dispersion instead of the optimum Raman gain and even so the length is normally deficient to attenuate the pump power [7].

1.2 Problem Statement

In literature, there are many researches focused on research and development in optical amplifiers systems. Nevertheless, the bandwidth of gain flatness was an affair in optical communications systems. Majorly, the gain that an optical amplifier introduces is dependent on the radiation frequencies of the energy bands. Consequently, by only two energy bonds for two types of amplifier the HFA can achieve wide gain. Many technics which include filters, FBG and DCF, can be used to enhance the bandwidth of gain flatness but this may lead to high cost, in order to solve this cost issue, we optimized the parameters of CSP-HFA utilizing high order Raman.

1.3 Objectives of the Research

1. To investigate the effect of CSP-HFA within the whole S/C/L band.
2. To design as well as enhances an efficient HFA using combined serial parallel architecture or composition, (CSP-HFA) in the S/C/L communication bands windows using pumping sources of higher order Raman scattering.

1.4 The Scope

The major objective of the study is to produce an effective HFA in the S/C/L band that is able to create a higher gain level using the dual-pump source with a wide amplification bandwidth, in order to achieve this goal, the research is split into three main categories as shown in Figure 1.1.

Different designs have been tested in order to ascertain the effect of the design metrics on the performance metrics of an EDFA, HFA and RFA. This work focuses on the impact of coupling ratio on the performance parameters of CSP-HFA. The effect of coupling factor of the input signal on a broadband CSP-HFA using multi-pump source is simulated and validated.

Optimization is the fundamental stage for this work design as well as performance evaluation. It focuses on ascertaining the pump power optimal values, coupling ratio and the wavelength of the pump in order to achieve an optimum performance for the gain, bandwidth, and noise figure.

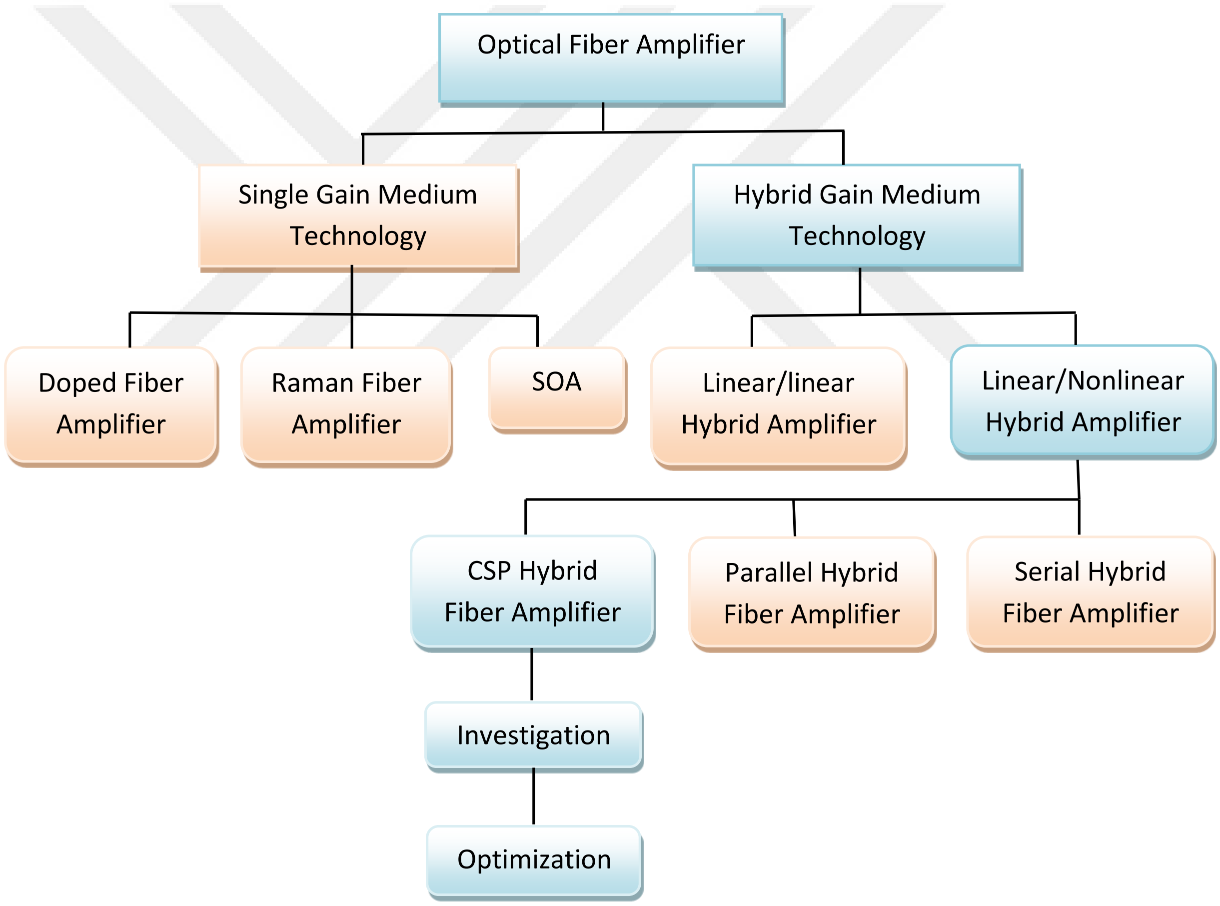

Figure 1.1 Scope of the research work

1.5 Literature Survey

In 1997, Paul F. Wysocki et. al., achieved 40 nm as a bandwidth of gain flatness with below 4 dB noise figure by using EDFA with grating filter; but as using high levels of filter loss, it would lead to high noise figure. Nevertheless, the output power of this model reaches nearly15 dBm with flat EDFA within 1 dB if the filter spectrum and fiber lengths were carefully chosen over 40 nm [5]. In 1998, Hiroji Masuda et. al., accomplished a highly usable bandwidth of 75 nm within range of (1531 nm to 1606 nm) by using two stages of EDFF's with an intermediate gain-equalizer and distributed Raman amplifier, besides distributed Raman amplifier include 85 km as a dispersion shifted fiber, therefore by using this design the WDM with 9 x2.5 Gb/s has been demonstrated successfully [8]. In 1999 Hiroji Masuda and Shingo Kawai achieved wide gain bandwidths of 80,76,69 nm with percentage of gain flatness of 11.3 %, 4.7 %, and 3.7 %, respectively, as well as acceptable noise figure below 6 dB and 13.8 dBm as a total output power. This model included one EDFA, which has a short fluoride-based on erbium-doped fiber and two isolated Raman fibers which pumped at three wavelengths simultaneously [6]. In the same year Shingo Kawai et. al., proposed a novel hybrid fiber amplifier consisted of distributed Raman amplifier and an erbium-doped fluoride fiber amplifier and they obtained over 67 nm within range of (1534-1601) nm with 1.5 dB as gain flatness [9].

In May 2000, Bumki Min et. al., proposed a novel design for C+L band communication windows by employing wide-band EDFA’s, the main idea for this design is utilizing the ASE from C-band EDFA and use it as an extra pump source for L-band. For large input signal -3.5 dBm, the gain spectra and noise figure were 2.6 dB and 0.6 dB respectively. This design consisted of two EDFA, the first is C-band EDFA with 20 m as a length is pumped by forward pumping at the wavelength of 980 nm with 90 mw, whereas the second is L-band EDFA with 300 m is pumped forward and backward with 53 mw and 57 mw respectively at the same wavelength 980 nm [10]. In 2003 Anna Pizzinat et. al., proposed a hybrid EDFA/DRA model, and demonstrated the effect of this design on high data rate RZ 4 40-Gb/s WDM system by using reliable simulation model, which takes into account the noise characteristics of the Raman amplifier. The nonlinearity distortion index has been minimized due to using intrinsic

Raman Amplifier; therefore, the performance of the system is enhanced such as keeping BER at the same level [11].

In July **2004 Chien-Hung Yeh** et. al., comprehensively researched about a conventional S to L-band EDFA module, that approximates to 120-nm gain bandwidth of between 1480 nm and 1600 nm, while applying coupled structure. In this work, a 32.8, 34.7, and 38.1 dB peak gain were achieved at 1504, 1532, and 1568 nm, respectively, with the input power at -30 dBm. Additionally, this amplifier gives a broad-band amplified spontaneous emission (ASE) light source of between 1480 nm and 1606 nm with an output level of about 40 dBm [12]. In **2005 Ju Han Lee** et. al., showed a compensation technic for dispersion Raman/erbium-doped fiber amplifier hybrid amplifier recycling residual Raman pump to increase the total efficiency for power conversion. This dispersion-compensating hybrid amplifier system possesses one pump source for Raman amplification in the DCF. The residual pump power after the DCF is reused for secondary amplification of the signal in an erbium-doped fiber connected to the DCF. Using this technic, they obtain a considerable increase in the signal gain and effective gain-bandwidth by approximately 15 dB and 20 nm respectively as compared to the Raman-only amplifier performance [7].

In **2008 S.K. Liaw** et. al., made A parallel-type, dispersion compensating C+L band erbium-doped fiber amplifier/Raman fiber amplifier by apportioning a mutual 1480-nm pump source. The gain spectra for C+L band are basically flattened by optimally apportioning the pump power ratio 1:29 for EDFA and RFA, respectively. For a signal input power of -20 dBm, the average gain is around 14 dB for the C-band EDFA and around 13.6 dB for the L-band RFA when a pump reflector is applied to reuse the residual pump power in L-band. In this case the noise figure is between 4.6 dB and 6.5 dB and the polarization gain is a bit less than 0.14 dB. Although, with the increase in the input power, the gain variation degrades to 4 dB and 6 dB at input power of the signal of -10 dBm and 0 dBm respectively [13]. In **2011 Ning Guo** et. al. suggested a new bi-directional hybrid fiber amplifier with a single-wavelength pump laser diode at 1495 nm. The hybrid amplifier is in theory used for bi-directional transmission for a 50 km bi-directional local area network (LAN) with 26ch×10 Gb/s. 13 C-band channels are used for downlink transmission while the other 13 L-band channels are used for uplink transmission. Four channels (with each band having two) are analyzed experimentally. Erbium doped fiber (EDF) amplifies the C-band channels whereas Raman amplification provides amplification for the L-band channels. It is worthy to note that the efficiency of the pump can be enhanced by applying a double-pass technic for both the EDFA and the RFA. There is a chromatic dispersion that is faced by all channels and can be compensated for by putting a fiber Bragg grating (FBG) array in reserved locations points on the segments of the dispersion compensating fiber (DCF). Furthermore, the gain equalization for all channels is obtained by varying the reflectivity of FBG. Simulation results and experimental measurements approve the posited feasibility of the device and its possible use in a bi-directional LAN [14]. In **February 2013 Simranjit Singh and R. S. Kaler** vividly showed an effective gain-flattened L-band optical amplifier while applying a hybrid configuration of a disseminated Raman amplifier (DRA) and an EDFA of a 160×10-Gb/s dense wavelength division multiplexed system at 25-GHz interval. With power of the input signal at 3 mW, a flat gain of greater than 10 dB was achieved throughout 187 to 190.975 THz having a gain variation of less than 4.5 dB while not using gain-flattening technics. The power achieved at the output at 3-mW input power was also ideally high whereby it was greater than 8.9 dBm and it was the highest ever noted for a DRA–EDFA hybrid optical amplifier with reduced channel spacing [15].

In **2014, Hardeep singh and Sukhwinder singh** researched on Raman-EDFA and Raman-SOA performance as well as EDFA-SOA hybrid amplifiers performance for 120 channel WDM systems. Each channel had a data rate 10 Gbps with a reduced channel spacing of about 50 GHz. The performances of these amplifiers were contrasted on the basis of dissimilar fiber lengths at 2 ps/nm/km dispersion of BER, Q-factor as well as Eye opening. They demonstrated that RAMAN – EDFA had a higher Q-factor and a lower BER. RAMAN – EDFA is the best option as compared to RAMAN-SOA and EDFA-SOA for higher capacity WDM systems having reduced channel spacing [16]. In December **2014, Mudhafar Hussein Ali** et. al., simulated a parallel hybrid fiber amplifier for the C+L-band using a gain controlling technic. In his work, he used an adjustable optical coupler to control the power of the input signal for both the EDFA and the RFA. The gain spectra of the C+L-band are essentially flattened by optimization of the coupling ratio for the power of the input signal. In a bid to improve the conversion efficiency of pump, he pumped EDFA branch using the residual Raman pump power. A gain bandwidth of 60 nm (1530 nm to 1590 nm) was achieved with the power of the input signal less than -5 dBm. The gain variation was approximately 1.06 dB at an input signal power of -30 dBm. It was eventually reduced to 0.77 dB when the input signal power was -5 dBm. However, its noteworthy that if a comb from a WDM transmitter is used, the system incurs some dispersion in the EDF branch [2].

In **2015 M. H. Ali** et. al., showed simulation results and an experimental validation for a wideband serial hybrid Raman/EDF amplifier. There were two configurations adopted. In configuration A, a Raman amplifier acted as the first stage, whereas in configuration B, an erbium-doped fiber amplifier was the first stage. For lower input signal power, the mean gain level was 20 dB having a 40 nm flat gain bandwidth for both configurations. In configuration B, the noise figure was prevailed by the EDFA and brings about flatter spectra and lower values than in configuration A. The posited hybrid amplifiers gain is basically affected by the second amplification stage [17]. In **2016 Shivani Radha Sharma and Vivek Ruder Sharma** demonstrated an effective model of a gain flattened hybrid optical amplifier having an EDFA/ RFA for 20×50Gb/s WDM system. This configuration possesses features of both amplifiers. The wavelength for optimization is from 1569 nm to 1577 nm, and this is in the C-band of optical communications to have a uniform gain with a low noise figure. Amplifier gain and noise figure are the most significant features of any amplifier and are used to gauge its performance. There are also other metrics on which the gain of an optical amplifier is contingent. These include the pump power and wavelength, fiber length, and the number of channels. Nonetheless, if these parameters are optimized in Optisystem software the maximum gain is 22.81 dB with 7 dB as a NF and 2.79d B of gain variation [18].

In the same year **Bagga, Parveen and Sarangal, Himali** researched about the 16 channel and 32 channel DWDM systems of hybrid amplifiers at 20 Gbps. The system performance was analyzed according to the transmission distance. The Q-factor and BER for the two hybrid amplifiers EDFA+RAMAN and RAMAN+EDFA at different transmission distance were compared. It was showed that a 16 × 20 Gbps and 32×20 Gbps DWDM system applying EDFA+RAMAN gave more effective results than a DWDM system using RAMAN+EDFA. The system was analyzed using OptiSystem 7.0 simulator. In **2017 Abdallah M. Hassan** et. al., gave an analysis of the Raman amplifier performance and different hybrid optical amplifiers (Raman-EDFA, EDFA-Raman). This configuration has 16 channels with a speed of 10 Gb/s. It can be clearly seen that EDFA-Raman demonstrated improved performance in regards to gain, lower noise figure, higher Q factor as well as bit error rate(BER) [19]. Again in 2017, **S. Tahhan** et. al. made a simulation analysis of long-haul (120 km) system (DWDM) of 32 channels at 40-Gb/s speed with 50GHz spacing for duo-binary return-to-zero modulation schemes. In his work, he analyzed both the Pre-and post-dispersion compensation technics using DCF and FBG and compared them at a high bit rate. The Q-factor and BER values were used to gauge the system response as a function of input power. The pre-FBG technic showed a better performance with regards to Q-factor that was about 11.5 at 0 dBm power of the input signal [20].

1.6 Thesis Outline

This thesis offers a simulation, design optimization and performance evaluation of CSP-HFA in the (S+C+L) band region. This thesis consists of five chapters, which are arranged as follows:

Chapter 1 presents a brief background information on optical communication systems and amplifier. Even so, it discusses the objectives of the research and the literature survey.

Chapter 2 A thorough discussion about optical amplifiers that include the EDFA, the RFA and the HFA is given in this chapter. Also, it discusses the dispersion and the ways to reduce it by dispersion shifted fibers (DSF), DCF, FBG. This chapter also discusses WDM techniques and its performance parameters.

Chapter 3 The methodology used for simulation is exposited in this chapter in addition to the design parameters. The major performance parameters are defined and investigated. And the effect of cascading amplification stages on these performance parameters of the CSP-HFA.

Chapter 4 Discusses the simulation results of pump power optimization, pump wavelength optimization, coupling ratio optimization, gain profile, noise figure and the saturation of the CSP-HFA system utilizing DCF.

Chapter 5 summarizes the major conclusions based on the achieved results.

CHAPTER 2

THEORETICAL BACKGROUND

2.1 Introduction

The communications world was enlivened by the genesis of telecommunications in 1870s. For a spate of years, co-axial cables and metallic cables with twisted wire cables, were used with frequencies of around 10 MHz and the system effective performance would degrade above this figure. Nevertheless, with an increase in the need for telephones, it was essential to ascertain an alternative to telephony to match with the increasing demand. The evolution of low-loss optical fibers solved this problem. Optical fibers have become indispensable for high-speed communication systems because of their enormous capacity, wide bandwidth and tremendous low loss. However, optical transmission performance is constrained by factors like scattering, non- linearity, attenuation, dispersion, etc. that affect the signal level. To compensate for the aforementioned constraints, there's need for signal regeneration within the transmission link after a certain distance and this can be achieved by employing optical amplifiers or repeaters in which the optical signal is converted to an electric signal, thereby amplified and then re-converted to an optical signal. Nonetheless, using repeaters to regenerate a signal, is a traditional way for loss compensation in the transmission link. These regenerators become rather expensive and more so complex DWDM light wave systems. The process is well-suited for controlled speed single wavelength operation and can be reasonably expensive for relatively high-speed multi-wavelength systems. Even so, these repeaters can hardly be upgraded to high bit rates once installed. Hence, much effort has been put into developing amplifiers that are "all optical". Such devices operate effectively in the optical domain to amplify the signal power level. Throughout, ages of communication systems with optical fiber, the conception of optical amplifier was a significant milestone. An optical signal can be amplified directly by these optical amplifiers without first being converting to an electrical signal. Optical amplifiers were first developed in the early eighties and employed in long haul communication systems in the late nineties. They were flexible, which helped to overcome the electrical constraint of an electric repeater, which was ideally unable to transmit at high bit rates. The opto-electronic repeaters rendered a maximum of 40-80 Gb/s bit rate[21]. This chapter gives the theoretical background of an HFA which is a combination of two gain media to expand the gain bandwidth as well as enhance the gain flatness.

2.2 Optical Amplifier

The optical signal in communication transmission systems can be amplified without convert it into other form by using optical amplifier. The Optical amplifier is playing an important role in optical communications and laser physics, the basic structure of an optical amplifier is shown in Figure 2.1 [22].

2.2.1 Review of an Optical Amplifier

Stimulated emission is the main principle of optical amplifier operation. Additionally, the level of the signal can be increased by optical amplifier over this operation. The stimulated emission mechanism is similar to that of lasers. Laser diodes needed for fiber amplifier are considered as the pumping source used to produce population inversion required for gain [23].

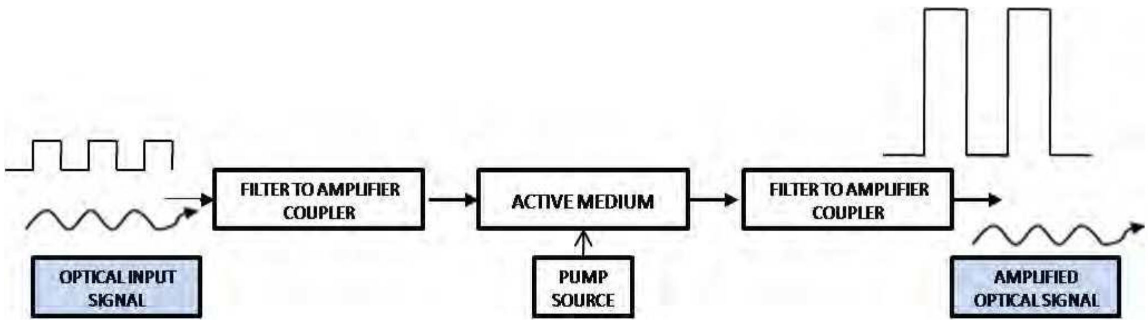

Figure 2.1 Basic structure of an optical amplifier [21]

2.2.2 Classes of Optical Amplifiers

Optical amplifiers have many applications ranging from ultra-long undersea links to short links in access networks; and it can be classified into three classes:

• In-line amplifier

• Pre-amplifier

• Post –amplifier

In-line amplifier: this class of optical amplifier works as a repeater along the link of fiber optic every 80-100km. furthermore, the transmission loss and the long distance between regenerative repeaters can be compensated by using this amplifier, as shown in Figure 2.2.

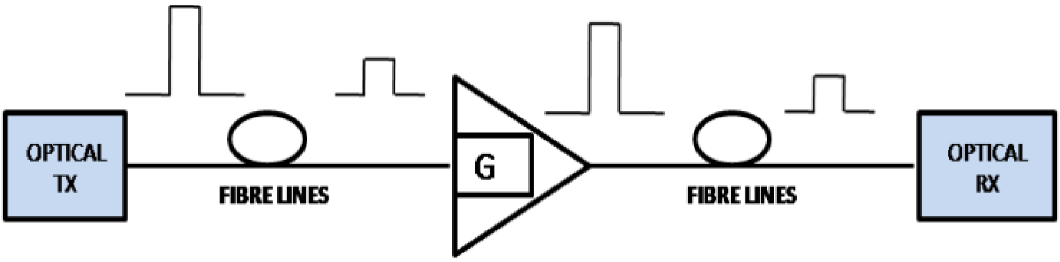

Figure 2.2 Optical amplifier as in-line amplifier [21]

Pre-amplifier: This class of optical amplifier used at the receiver and before the photo detector in order to reinforce the weak received signal, therefore, the sensitivity of the photo detector will increase by effectively. This configuration is shown in Figure 2.3.

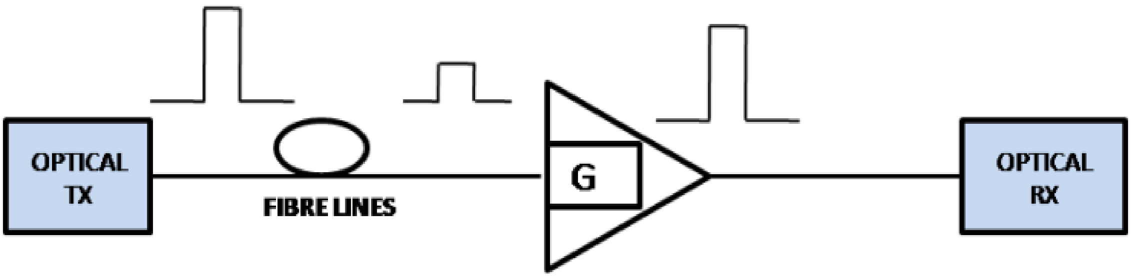

Figure 2.3 Optical amplifier as preamplifier [21].

Post-amplifier: This class of optical amplifier used at the end of transmitting in each DWDM communication system. Normally, this class produces low gain and high output power and it works in saturation region. The power launched into the fiber link is improved and therefore the distance between the repeaters can be expanded and according to amplifier gain and fiber loss, the transmission distance can be increased by 10-100 km, the Post-amplifier is shown in Figure 2.4 [21].

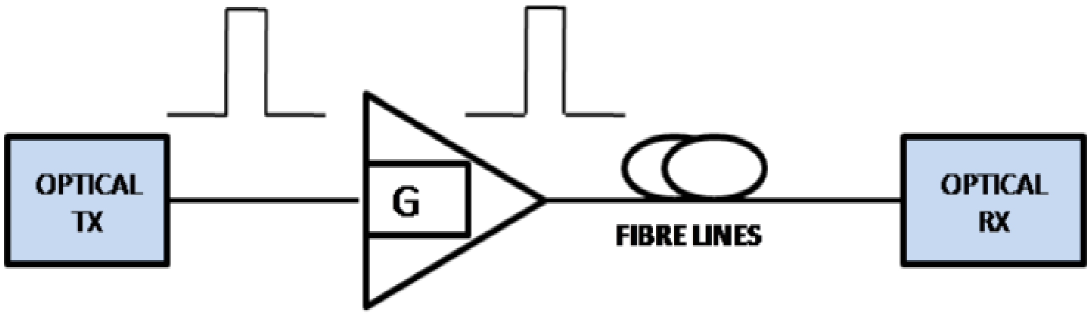

Figure 2.4 Optical amplifier as post amplifier [21].

2.2.3 Types of Optical Amplifiers

The optical amplifiers which found widespread use in communication systems can be classified into three categories: -

1. Raman Fiber Amplifier (RFA)

2. Erbium Doped Fiber Amplifier (EDFA)

3. Semiconductor Optical Amplifier (SOA)

The first two types, RFA and EDFA can be efficiently coupled to the transmission fiber by splicing with a minimum coupling loss. Since the EDFA needs low power for pumping, it can obtain from semiconductor laser diodes easily. Table 1.1 shows the basic difference between the two optical amplifiers [23].

Table 1.1 Difference of materials and operating bandwidth of two optical amplifiers [21].

Type of optical amplifier	Material required	Operating Working band
Erbium Doped Fiber Amplifier (EDFA)	Lightly doping silica or Tellurite with rare earth element, i.e. Erbium	O-Band, S-Band, C-Band and L-Band
Raman Fiber Amplifier (RFA)	Raman Lasers	All Operating Bands

Optical fiber amplifiers are used for insertion loss, distribution loss, and optical fiber attenuation compensation in the nodes of a WDM optical network. These losses can also be compensated by using optical amplifiers. The incident light in the amplifier's gain medium can be amplified by using stimulated emission of a number of meters for an EDFA, this kind of amplifier called the linear-gain amplifier [24]. Conversely, the nonlinear-gain amplifier amplifies the weak signal over lots of kilometers of RFA. The photons can be generated by “Raman Scattering” of incident light within the lattice of the medium of gain and these generated photons are coherent with the incoming photons [25].

2.3 Erbium Doped Fiber Amplifier

The EDFA could be the most widely applied amplifier in optical communication and this is owed to its compatibility. Its main features are; Erbium-doped fiber (EDF), optical isolators, laser source, couplers to aggregate the pump wavelengths and the signal, and optical filters. The optimum length of the optical fiber is characterized by the power of the incoming signal, pumping wavelength, erbium doping and pump power [26]. An EDFA has got a comparatively broad wavelengths range and this makes it ideally effective for amplification in a WDM system. Theoretically, an EDFA can amplify wavelengths of 1500 nm to 1600 nm. Nevertheless, realistically, two communication windows are prevalent (C and L) and in this case a signal can stimulate the excited atoms and eject photons [27].

2.3.1 Advantages of EDFA

EDFAs are undoubtedly the best option for optical amplification in today’s light wave systems. Erbium is used as a dopant into glass host (fiber) and the doped fiber is used as the amplifying medium. The amplified output of an EDFA is around 1550nm and its widely used in DWDM transmission systems.
EDFAs are inspiring light wave systems by enhancing the network performance and reducing costs.

2.3.2 Working Principle of EDFA

The Er3+ ion acts as a three-stage system, where the main players are the 4I 15/2 ground state, the 4I 13/2 first excited level and the 4I 11/2second excited level. The diagram for the energy level of Er3+ is shown in Figure 2.5.

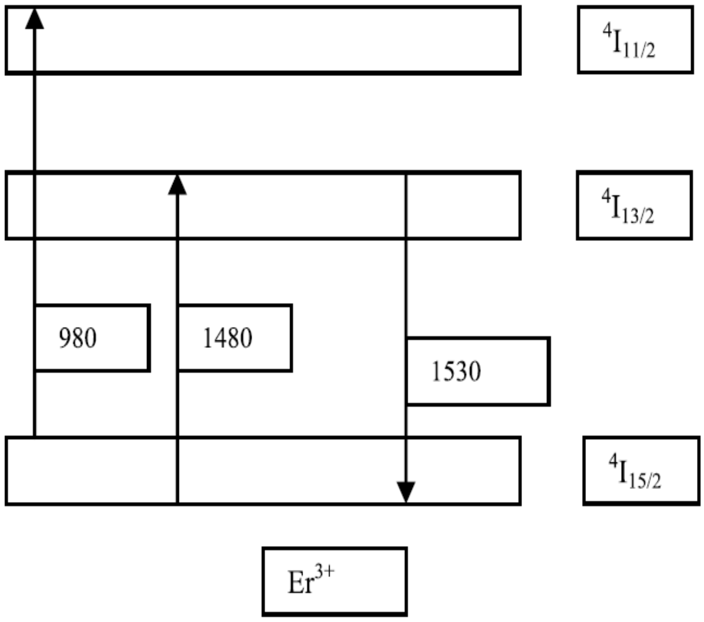

Figure 2.5 Energy Level Diagram of Er3+ [21].

EDFAs are of peculiar stake in telecommunications, and this is due to their emission spectrum showing a 20-dB gain and above between 1530 nm-1560 nm and even so the third window in optical communication. The absorption spectrum shows that excellent absorption takes place around 380, 520, 800, 980 and 1480 nm as shown in Figure 2.6. At shorter wavelengths the absorption bands are not required because of the unavailability of semiconductor laser diodes. At 980 nm and 1480 nm, efficient laser diodes are readily available which are hence applied as pump sources [28].

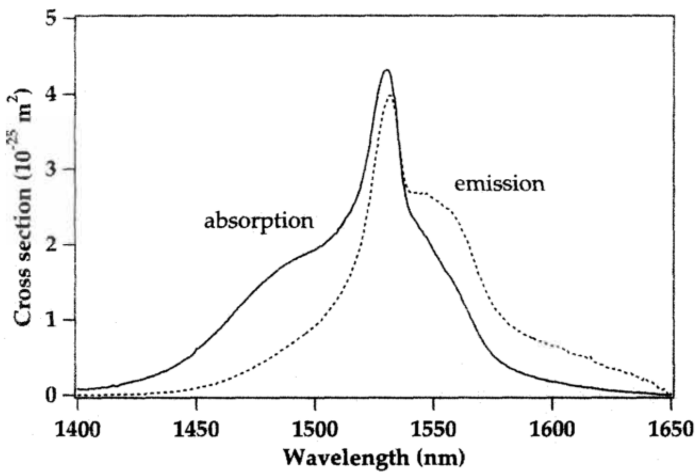

Figure 2.6 Absorption and Emission Spectra of EDFA [28].

The signal power level is inversely proportional to the gain coefficient, which is ordinarily common in laser and amplifier systems. This is largely due to the de-population of level 2 from the high number of signal photons. The gain coefficient can be;

$$g = \frac{g_0}{1+\frac{P}{P_s}} \tag{2.1}$$

where g_0 is the gain coefficient for the small signal at a specific wavelength, P is the power level for the signal and P_s is the power level for the saturated signal, required for a 3 dB gain-drop [29].

2.3.3 Limitations of EDFA

The major drawbacks for an EDFA is the spectral subjectivity of the gain of the amplifier. Thus, varying channels for DWDM systems are amplified differently. These constraints become severer in long-haul systems, where a chain of EDFAs is employed. An EDFA has a peak gain at 1530 nm, above which the gain slightly degrades and stays flat till 1550 nm after which it reduces sharply.

Hence, EDFAs are mostly applied in the C-band (1530 nm-1560 nm) for optical communication systems [21].

2.3.4 EDFA Noise

An explanation for the EDFA amplified spontaneous emission (ASE) noise is given below and noise figure elucidation.

2.3.4.1 Amplified Spontaneous Emission Noise

The fact that noise is apparent in almost all amplification systems based on atomic population inversion may be well comprehended by the physical picture of amplified spontaneous emission. The noise photons randomly emitted by the spontaneous decomposition of excited atoms are negligible as compared to the stimulated emission due to the presence of many signal photons (stimulating photons).

However, with the signal and noise travelling along the doped fiber, the spontaneous emission, and the stimulated emission are both amplified. The amount of noise power in a single mode within a given bandwidth (*dv*) is [30].

$$\boldsymbol{p = hvn_{sp}(G(v) - 1)dv} \quad \textbf{(2.2)}$$

This depicts that the noise power is proportional to *nsp* and gain

2.3.4.2 Noise Figure

In Equation (2.2), the noise power may not give info on the performance of the system and the constraining factor for the detection system is the SNR. Because of this, it is the *NF* that is widely used to characterize the noise in the amplification system, and is defined as [24]:

$$\boldsymbol{NF_{EDFA} = \frac{(SNR_{in})}{(SNR)_{out}}} \quad \textbf{(2.3)}$$

Where: NF_{EDFA} is the noise figure of the EDFA, $(SNR)_{in}$ and $(SNR)_{out}$ are input and the output signal to noise ratio respectively.

2.4 Raman Fiber Amplifier

Transforming a trivial divide of incident light power to scattered light is known as spontaneous Raman scattering. The concept was found out in 1928 by C. V. Raman [31]. In general, the scattered light frequency differs from that of incident light by the vibrational degrees for the medium. Its noteworthy that spontaneous Raman scattering is a weak process. As an example, whenever light travels in a 1 cm^3 medium, only a small percentage of the billions of the incident light is scattered in the Stokes frequency. Although, if a laser source that is acute is incident on a particular molecular medium, a higher scattering component can prevail. Even so, 10% or more of the incident power is transferable to the scattering parts. This nonlinear scattering re-known as the stimulated Raman scattering (SRS) was found in 1962 [32]. Firstly, Raman gain is found in every fiber, which is cost–effective. Secondly, the gain is not resonant, and is over the whole transparent fiber region. Thirdly, the gain spectrum of the Raman amplifiers can be adjusted by the wavelengths of the pumps. As an example, a spate of pump lines may be applied to enlarge the optical bandwidth. Even so, the distribution of the pump can determine how flat the gain is. Lastly, Raman amplifiers are somewhat broadband amplifiers, having a bandwidth of 5 THz and above, and the gain is considerably flat over a wider bracket of wavelengths.

2.4.1 Working Principle of RFA

The SRS can significantly convert optical fibers to Raman amplifiers that are of wideband and Raman fiber lasers which are tunable. It can also ideally set the WDM system's performance by moving some power from between varying wavelengths [33]. Herein, the incidental light is the pump source, and is known as the Raman pump power (RPP), whereas the transmitted power is the residue. The scattering parts converted to lower frequencies, are Stokes waves, whereas the parts converted to higher frequencies (blue–shift) can be called as anti–Stokes waves [33][34].

The Stokes generation is owed to the energy exchange by the photons and the molecules of material. The incident photon charges up a molecule from to the virtual state and then the molecule returns to the vibrational state and a Stokes photon is given out. There's a smaller amount of energy between the virtual and the vibrational states than between the ground and the virtual states and this results in photons having longer wavelengths. Conversely, within the process of the anti–Stokes, the excited molecule is within the vibrational level. Thus, the anti–Stokes signal frequency is higher than that of the incident photon.

Moreover, Stokes waves intensity is tremendously hiked up more than the anti–Stokes waves intensity and because the anti–Stokes process needs the vibrational state to be primarily having a photon of required energy and momentum. Thereafter, the anti–Stokes process was disregarded, since it plays a peanut role in Raman amplification. The quantum–mechanical energy diagram for Raman scattering in the Stokes generation process is shown in Figure 2.7.

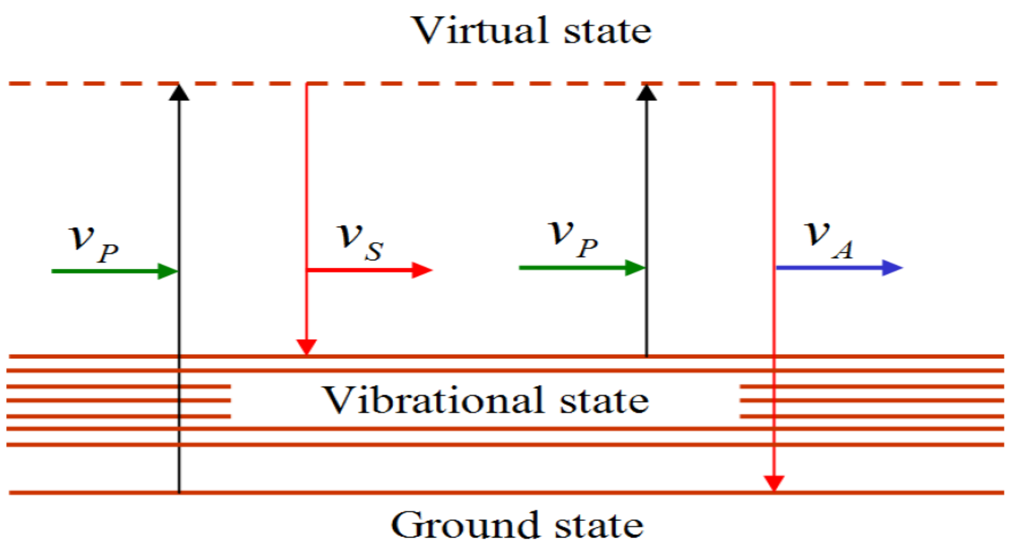

Figure 2.7 Quantum–mechanical energy diagram for Raman scattering[33].

2.4.2 Gain Spectrum and Gain Saturation

The coefficient of the Raman gain is the fundamental parameter that characterizes the spectrum of the Raman gain, and more so it is related to the spontaneous Raman scattering cross-section. Additionally, the increase in the Stokes power via the SRS can be depicted with this gain. For a bare approach that is rendered true for CW and quasi–CW conditions, initially the increase in the Stokes power is given by [35].

$$\frac{dP_S}{dz} = g_R P_P P_S \tag{2.4}$$

Where P_s is the Stokes power and P_p is the pump power.

The coefficient of the Raman gain for silica fibers was ascertained in the other SRS experiments [36].

In general terms, it depends on the optical fiber composition. The Raman gain spectrum in silica fibers stretches up to 40 THz having a broader peak at about 13 THz and is because of the silica glass amorphous nature [37].

The gain of the signal depends largely on the frequency difference and it is at its highest if the signal beam is basically downshifted from the frequency of the pump by 13.2 THz. This approximates to 100 nm in the regime of 15xx nm [38]. The Raman gain is prevalent in all the spectral regions in that optical fibers can be suitably used for any signal amplification if a good pump source is employed. The pump parallel to the signal is the co– or forward–pump, while that opposite is the counter or back-ward pump. When the fiber is pumped, the two points are connected by the actual transmission span; this setup is called the distributed Raman amplifier. The amplifier is a discrete Raman amplifier if it's in the box at either the transmitter or the receiver, it is known as. Another difference is the fiber length. Ideally, distributed Raman amplifiers are more than 40 km long, while discrete Raman amplifiers are 5 km long. This may result in some differing considerations. The schematic of an optical communication system employing Raman amplification is shown in Figure 2.8.

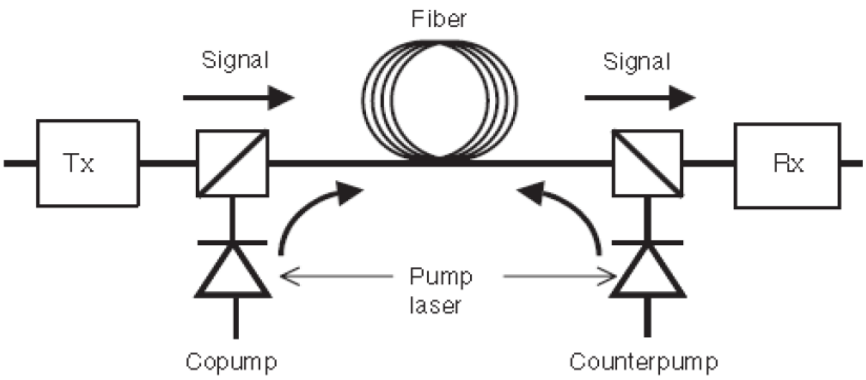

Figure 2.8 Schematic of an optical communication system employing Raman amplification [31].

The pump power, Pp, and the signal power, Ps, along the lengthwise axis of the fiber in a Raman amplified may be depicted as [31]:

$$\frac{dP_S}{dz} = g_R P_P P_S - \alpha_S P_S \quad (2.5)$$

$$\xi \frac{dP_P}{dz} = \frac{\omega_P}{\omega_S} g_R P_P P_S - \alpha_P P_P \quad (2.6)$$

Where g_R ($W^{-1}m^{-1}$) is the normalized coefficient of the Raman gain of the fiber in regard to fiber effective area (*Aeff*), α_s andα_p are the signal and pump attenuation coefficients respectively and ωs and ωp are their respective angular frequencies. The parameter ξ takes values of ±1, depending on the pumping configuration; the minus sign is used for backward–pumping. In both equations, the first term depicts the SRS signal gain and the second term depicts the intrinsic pump loss. In case the depletion of the pump by the signal is not considered, Equation (2.6) can be solved for the forward propagating case to give $P_P(z) = P_0 \exp(-\alpha_P z)$

Where P_0 is the input pump power at z=0, this result is substituted into Equation (2.5), and the resulting differential equation may be analytically solved to give:

$$\boldsymbol{P_S(L) = P_S(0)\exp\left(g_R P_0 L_{eff} - \alpha_S L\right) \equiv G_N(L) P_S(0)} \quad \textbf{(2.7)}$$

$$\boldsymbol{L_{eff} = [1 - \exp(-\alpha_P L)]/\alpha_P} \quad \textbf{(2.8)}$$

Where G_N is the net gain and L is the fiber length. In distinctive transmission fibers, the loss is around 0.25 dB/km at 1455 nm and hence, L_{eff} for the pump light is around 17 km for spans beyond 60 km.

Where G_N is the net gain and L is the fiber length. In distinctive transmission fibers, the loss is around 0.25 dB/km at 1455 nm and hence, L_{eff} for the pump light is around 17 km for spans beyond 60 km.

The RFA has classifiable features as compared to the conventional EDFA, like wider bandwidth, low noise figure, as well as lower non-linear effect. Although, the saturation of the gain resulting from SBS is vital, and thus many researchers are critically investigating this effect [38][39][40]. When the power of the signal increases, the amplifier gain is similar at first, and then it decreases. Gain saturation is very important and fundamental in optical communication systems. With a signal with a particular wavelength being coupled to a DWDM system, the gain of RFA changes apace if the signal power goes beyond the saturation power, and this requires to be averted. Hence, it is essential for designers to know the saturation power and ascertain what gain is saturation depending on [41].

In RFAs, for cases where the incident signal surpasses the threshold of SBS, most power gets channeled to the Stokes light that is backscattered. The SBS threshold can be [34]:

$$\boldsymbol{P_{SBS-th} = \frac{21 A_{eff}}{g_B L_{eff}}} \quad \textbf{(2.9)}$$

Where g_B is the Brillouin gain peak value, A_{eff} is the fiber core effective area. If there is no pump light, Equation (2.7) can

$$\mathbf{P_s(L) = P_s(0)exp(-\alpha_s L)} \qquad \textbf{(2.10)}$$

Thus, we get the RFA on/off gain (G_A) for a mild signal with (2.7) and (2.10) as:

$$\boldsymbol{G_A = exp\left(g_R \frac{P_0}{A_{eff}} L_{eff}\right)} \qquad \textbf{(2.11)}$$

And if P_s is mild enough, G_A doesn't change and is almost invariable. However, if P_s is larger to even the extent of saturation power, g_R begins to change. And if P_s gets to the threshold in (2.9), then SBS occurs, causing a gain decrease. In this case g_R can be:

$$\boldsymbol{g_R = \frac{g_0}{1+P_s/P_{sat}}} \qquad \textbf{(2.12)}$$

Where g_0 is the coefficient of maximum gain and the saturation power is P_{sat}. If the fiber attenuation coefficient is included, the distributed signal power is then [42]:

$$\boldsymbol{\frac{dP_s}{dz} = g_R P_s = \frac{g_0}{1+P_s/P_{sat}} P_s} \qquad \textbf{(2.13)}$$

Where g_0 is pump power. Evidently, equation (2.13) can be integrated and using$P_s(L) = GP_s(0)$, the saturation gain becomes:

$$\boldsymbol{G = G_0 exp\left[(1-G)\frac{P_s(0)}{P_{sat}}\right]} \qquad \textbf{(2.14)}$$

Where G_0 is the small signal gain.

2.4.3 The Noise of Raman Fiber Amplifier

The RFA effective performance is largely impacted by noise. Moreover, in RFAs, the three major noise sources are elucidated below:

2.4.3.1 Spontaneous Raman Scattering

This is aggregated to the signal that is amplified and behaves as noise due to the random phases in photons that are spontaneously generated [43].This noise mechanism reflects spontaneous emission that influences the EDFA performance, apart from the Raman, wherein it depends on the photon's population when in vibrational state, and is in turn reliant on the Raman amplifier temperature. Furthermore, the conception of the signal with the noise added by spontaneous Raman scattering should also be considered.

However, practically, the only noise present is that surpasses the amplifier bandwidth and can be repressed by putting an optical filter at the output of the amplifier. In this case the total ASE power after the RFA can be given by [31]:

$$\mathbf{P_{ASE} = 2S_{ASE}B_{opt}} \tag{2.15}$$

Where B_{opt} is the bandwidth of the optical filter.

S_{ASE} is the spectral density of the ASE and is:

$$S_{ASE} = n_{SP} h v_0 g_R G(L) \int_0^L \frac{P_P(Z)}{G(Z)} dz \tag{2.16}$$

Where n_{sp} is the factor for spontaneous scattering and hv_0 is the average photon energy.

2.4.3.2 Rayleigh Backscattering

The performance of distributed Raman amplifiers majorly limited by Rayleigh backscattering [44][45], and is the most salient loss mechanism in all fibers. Though most of the scattered light gets out through the cladding, save the backscattered light that can couple into the core mode that is supported by a single mode fiber. This backward propagating noise is in most cases not considered, since its power level is lower by more than 40 dB as compared to the forward–propagating signal power.

Nonetheless, it can possibly be amplified over longer fibers with the use of distributed Raman gain. Rayleigh backscattering influences Raman amplifiers performance in two manners. First, it a part of a backward–propagating ASE can be in the forward direction, which can ideally cause an improvement on the overall noise. Although, this noise is relatively very small, and may not significantly affect the Raman amplifier. Second, the double Rayleigh backscattering gives rise to some crosstalk element in forward-direction, whose same spectral range is the same as of the signal of interest. The noise induced by Rayleigh is amplified with the Raman gain, thereby becoming the main power penalty source in most of such systems [31].Figure 2.9 illustrates the schematic of signal double-Rayleigh backscattering. The fluctuations in density at z2 in the transmission fiber can reflect a mild portion of the signal. The field that is backward–propagating is reflected again by fluctuations in density at z1, thenceforth propagating in similar direction with the signal. It should be noted that z1 and z2 may change over the whole fiber, thus the total noise can be got by summing up all the paths. It's for this that the Rayleigh noise is sometimes taken to be arising from multi–path interference [46].

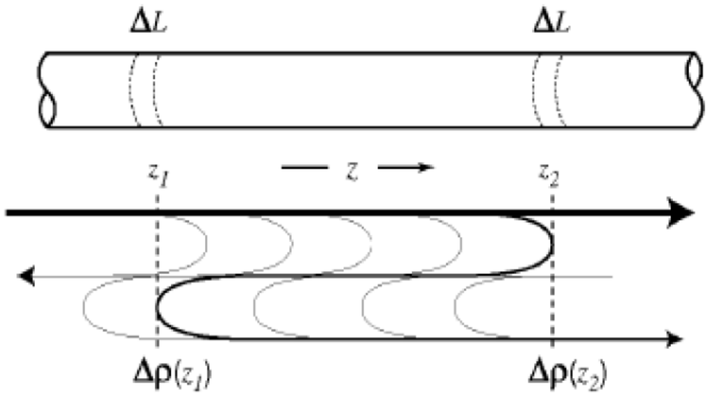

Figure 2.9 Schematic illustration of double Rayleigh backscattering in distributed Raman amplifiers. The signal is first reflected at z2 and then again at z1 through local density fluctuations Δρ at these two locations [46].

2.4.4 Pump–Noise Transfer

It should be noted that lasers have some kind of fluctuations in their intensities. This may be worse in case of semiconductor lasers that is used to pump Raman amplifiers because the power fluctuations in those kinds of lasers are relatively higher from and may result in enormous spontaneous emission rates. As depicted from (2.7), the gain in Raman amplifiers depends on the pump exponential power. Therefore, it can be deduced from that any changes in the pump power, results in a relatively larger change in the power of the amplified signal and in this case, the noise source is referred to as the pump–noise transfer. The noise transfer depends on a number of factors that include the pumping scheme, amplifier length, and the fiber dispersion characteristics.

The fluctuations in power of semiconductor lasers are measured via a frequency dependent quantity known as the relative intensity noise (RIN). The RIN value constitutes the intensity spectrum and/or power fluctuations [46].

2.5 Pumping Configuration

The light of the pump may be fed from either the front and/or the back of an EDF. It's injected in that it travels in the signal light direction, and that is known as forward-pumping. It may be also fed in the opposite way and is known as backward-pumping. Needful to note is that there is also the bidirectional pumping that aggregates the forward and backward pumping. It should also be noted that the pump light is always attenuated as it propagates.

With forward pumping, as illustrated in Figure 2.10 (a), N2 –N1/N is at its peak at the input of the fiber. This implies that the population inversion factor is relatively smaller at the input, thus, the ASE noise is lower at the input. When amplifiers with dissimilar noise figures are being cascaded, the total noise performance is more effective if the lower-noise amplifier is in front of the noisier. Hence, forward-pumping is more effective than backward-pumping in noise performance. For backward pumping, the power for the saturation signal is higher than for forward-pumping. At the amplifier fiber endpoint, the intensity of the signal is higher as well as very closer to saturation. For the case of backward pumping, it is at the endpoint of the fiber that the pump-power is highest, where a higher intensity is required to raise up the power for the saturation signal. Notably, even the total gain of the amplifier is increased. The gain may saturate, and the overall power reduce there's no adequate pump power. Hence, backward-pumping boasts of high saturation power as well as high gain. In conclusion, bi-directional pumping, as illustrated in Figure 2.10 (c) enjoys the merits of both though at complexity cost.

In Figure 2.10 the pump light from 1.48µm laser diode is being mated to the path of a 1.55µm light signal with the use a dichroic mirror. This mirror is of dielectric film layers with thicknesses that can pass via the 1.55 µm light signal and reflect the 1.48 µm light signal. Since optical isolators, are ideally insensitive to the polarization of light signal but rather to the direction of propagation, they are put on both fiber endpoints to prevent the reflected wave to get back into the fiber. An optical filter is also put at the end of the amplifier to bar the pump light from getting out and get rid of ASE noise in the used detector and in this case, a narrowband filter (<1 nm) is required [47].

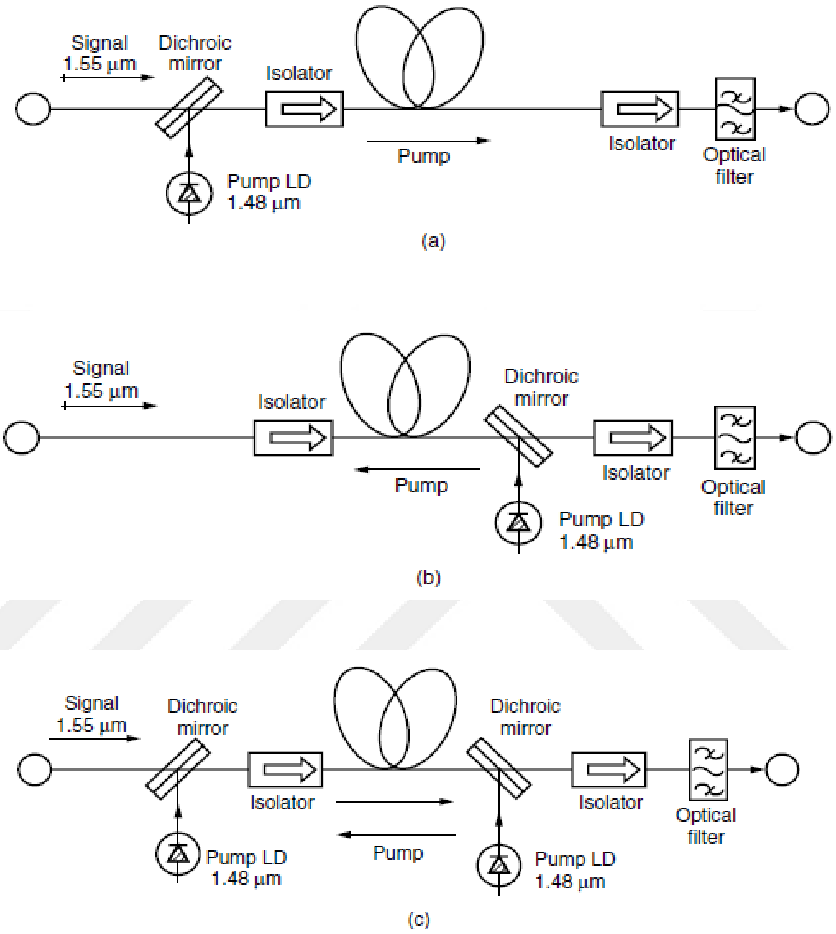

Figure 2.10 EDFA pumping configurations (a) Forward pumping (b) Backward pumping (c) Bidirectional pumping[47].

2.6 Hybrid Gain Medium Technology

Optical amplifiers are very essential in long–haul transmission systems, in that they normally compensate for fiber loss [33][48]. There are two re-known classes of optical amplifiers studied by many researchers namely; the EDFA and RFA [49][50]. The EDFA is primarily used between 1530 nm -1570 nm (C–band) and since this band is normally used in DWDM systems, EDFAs are inapplicable for this purpose.

The length of EDFA may be enhanced as an immediate solution to shift the amplifier bandwidth up-to a wider band (L–band). Although, the approach needs a higher pump power as well as a lower gain and a higher NF in contrast to the former [51]. More so, HFA can increase the bandwidth and also the gain flatness. To realize an HFA, different gain mediums are merged, either both linearly or one linearly and the other nonlinearly.

2.6.1 Linear–Linear HFA

Implementing an HFA with multiple amplifiers having varying gain bandwidths may be the most effective approaches to enhance the gain bandwidth for an optical amplifier. These amplifiers may be cascaded in parallel and in series. When cascaded in parallel, the WDM signals at the amplifier input are first de-multiplexed into a spate of band groups of particular wavelengths using a WDM coupler, thereafter they are amplified using amplifiers with gains in the matching wavelength band. Then they are multiplexed using a WDM coupler. This configuration is quite simple. Additionally, it is flexible whereby you can begin with a single amplifier and cascade it with other numerous amplifiers depending on the capacity required. The examples for this configuration are the C/L band HFAs that combine the C and L band EDFAs and S + C + L band amplifiers that combine a S, C and L band thulium-doped fiber amplifiers (TDFA) [52].

2.6.2 Nonlinear–Linear HFA

The hybrid EDFA/Raman amplifier aggregates two gain media; the nonlinear RFA and the linear EDFA gain. Hybrid EDFA/Raman amplifiers are taken to be an enabling and assuring technology for prospective DWDM systems, as illustrated by conventional experimental studies [53].

HFAs are made to manipulate the span length, reduce on the handicaps by fiber non-linearities, enlarge the EDFA bandwidth, increase the overall signal gain and heighten the efficiency of pump-conversion [54][1]. This thesis focuses on hybrid Raman–EDF HFA.

2.7 Dispersion

Dispersion or distortion of light beam is caused by a number of factors. The fundamental contributing mechanisms include:

1. Chromatic (material) dispersion.
2. Waveguide dispersion.
3. Modal dispersion.

To comprehend the dispersion phenomenon, the group delay or group velocity related with the energy transmitted through the fiber must be as well regarded. The phase velocity can be depicted by equation (2.17).

$$\boldsymbol{u_{w=\frac{c}{n}}} \tag{2.17}$$

Where c is the light velocity in free space and n is the refractive index of the medium. If we consider a non-monochromatic source, source center wavelength can be used to determine the phase velocity in a dispersive medium. Although, it is normal to use the group velocity, ug. Group velocity is referred to as the velocity of the wave envelope and is the velocity at which modulated information on the wave propagates. In general, the group velocity and phase velocity of a wave in a dispersive medium is always different. The group velocity inverse is known as the group delay per unit length, χg. Group velocity and group delay can therefore be depicted as chromatic dispersion:

$$\boldsymbol{u_{g=\frac{c}{n_g}}} \tag{2.18}$$

And

$$\boldsymbol{\chi g = \frac{n_g}{c}} \tag{2.19}$$

Chromatic dispersion is sometimes called material dispersion and is as a result of the nonlinear wavelength variation with the refractive index of a material (change in n1 and n2 with respect to λ). A dielectric medium which has a refractive index that is a function of wavelength is referred to as a dispersive dielectric medium. Nonetheless, laser beams are not precisely monochromatic, and they generally stretch to a wide range of wavelengths. Hence, if the relationship between the refractive index and the wavelength is not linear over the specified range, different wavelengths propagates with varying velocities within the fiber, and this brings about distortion or interference of the optical signal. Thus, pulse broadening caused by chromatic dispersion in a single-mode fiber is depicted as:

$$\triangle \boldsymbol{\tau cd} = \frac{L_f}{c} \boldsymbol{\lambda} \frac{d^2 n}{d\lambda^2} \triangle \boldsymbol{\lambda} = L_{f \triangle\lambda D_d} \tag{2.20}$$

Where Dd is the dispersion coefficient in ps/(km.nm).

The chromatic dispersion effect can be suppressed by suitable selection of the beam wavelength to be in the region where $d^2n/d\lambda 2 \approx 0$. This is in most times in the range 1.2 µm – 1.4 µm for fused silica. It should be noted that the effect of chromatic dispersion in multimode fibers is always negligible. Although, it is the most salient class of distortion and hence constraints the bandwidth in single-mode fibers. Waveguide dispersion is caused by the fact that the propagating features of a particular mode always depend on the beam wavelength. Notably, wavelengths that are longer have a longer path because they can reflect at more oblique angles with the cladding. Pulse broadening, $\triangle\tau wd$, caused by waveguide dispersion can be depicted as:

$$\triangle \tau wd = \frac{L_f}{c} \frac{\triangle\lambda}{\lambda} (n2 - n1)\, D_w\ \nu_n \tag{2.21}$$

Where Dw(νn) is the dimensionless dispersion coefficient and L_f is the fiber length. The pulse broadening brought about by wave guide dispersion is ideally smaller as compared to chromatic dispersion. Inter-modal dispersion is as a result of differences in the distances over which propagation occurs by the various modes maintained by the fiber. The transient delay in the arrival times of the rays brings about delay distortions and/or change in the spectrum of the primary input beam. When a pulse of a laser gets into the fiber, it is divided up among the multiple guided modes in the fiber. The pulse therefore is divided up into a spate of pulses and each of them gets out of the fiber at a specific time owing to the difference in the delays of the modes. An elementary estimation of pulse broadening brought about by inter-modal distortion can be ascertained by the difference between the travel time of the fastest and slowest mode. This is depicted as:

$$\triangle \tau_m = t_{max} - t_{min} = \frac{\triangle n_1 \ L_f}{c} \tag{2.22}$$

It is clear that modal dispersion may in general not be a constraint with single-mode fibers because of the fact that single-mode fibers can only maintain one mode of the beam. Nevertheless, for the case of step-index multimode fibers, chromatic dispersion is relatively smaller than modal dispersion. Modal dispersion is the predominant type of distortion, and it primarily constrains step-index multimode fibers to lower bandwidth (less than 100 MHz km) applications [55]. This research focuses on material and waveguide dispersions which are the dominant types of dispersion in SMF.

2.7.1 Dispersion Compensation with DSF

In Figure 2.11, Material dispersion and waveguide dispersion, as well as their sum are plotted versus wavelength. The dispersion parameter, in ps/(nm.km), is used as to represent the dispersion. The unit depicts the number of picoseconds of spread in arrival time for a source wavelength spread of 1 nm and a fiber length of 1 kilometer. Thus, the waveguide dispersion continues to be an insignificant negative quantity throughout as illustrated in Figure 2.11. At a wavelength of 1.32 µm, the dispersion of the waveguide tends to cancel the material dispersion, thenceforth the single-mode optical fiber tends to be free from the two dispersions completely.

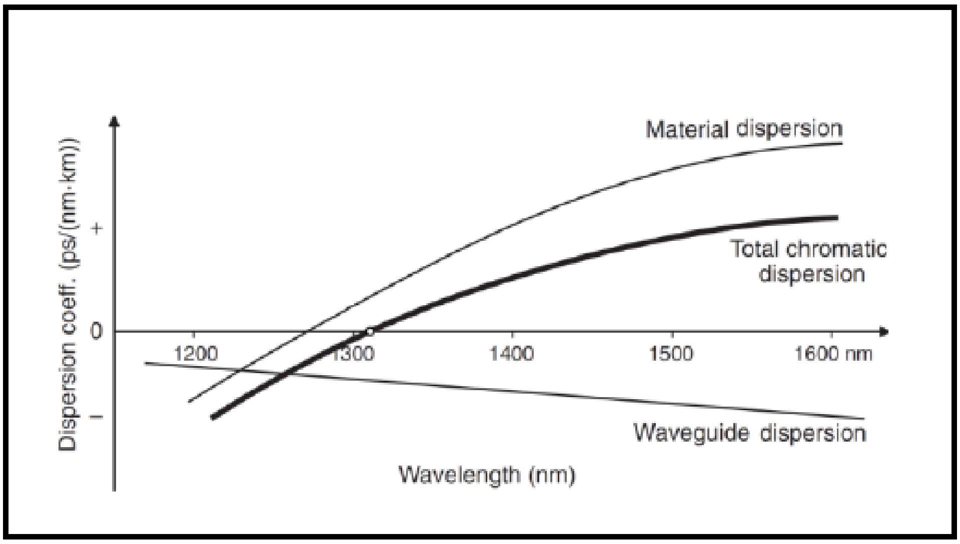

Figure 2.11 Dispersion of a single mode fiber

The dispersion-free transmission wavelength may be changed to longer wavelengths particularly to 1.55 µm, and this occurs if waveguide dispersion is enhanced. An optical fiber which has a dispersion free wavelength altered to the lowest loss wavelength and can have the advantages of no dispersion and low loss. That kind of a fiber is known as a dispersion-shifted fiber.

$$\boldsymbol{D = -\frac{\lambda}{C}\frac{d^2\, n_1}{d\,\lambda^2} - \frac{n_1 \triangle}{c\lambda} V \frac{d^2(Vb)}{dV^2}} \tag{2.23}$$

The second term in Eq. (2.23) gives the waveguide dispersion (Dw). The following are the ecumenical ways of increasing Dw for average step index configuration:

1. Select a value of V close to V =1.33, wherein Vd^2Vb/dV^2 is at maximum.
2. Increase the difference in the refraction indices (△ n1= n1 -n2) between the cladding glasses and the core. However excessive core doping to increase the refraction index is undesirable due to increased Rayleigh scattering loss [47].

2.7.2 Dispersion Compensation with FBG

Optical fibers are used in the quickly growing arena of fiber sensors. In spite of the advances in optical fiber manufacturing, it is still a challenge to incorporate optical components like mirrors, wavelength filters, and partial reflectors with fiber optics. Of recent, all this has greatly changed with the ability to change the core refraction index in a single-mode optical fiber by optical absorption of ultraviolet (UV) light. The optical fibers photosensitivity allows for the direct fabrication of phase structures into the fiber core, and this is known as the fiber Bragg grating. A fiber Bragg grating comprises of what is known as a periodic modulation of the refractive index in the core of single-mode optical fiber. The period of the refraction index variation is illustrated by Λ, the Schematic representation of a Bragg grating inscribed into the core of an optical fiber is shown in Figure 2.12. A broadband light is put into the fiber core. A portion of the input light is reflected, and the other portion is transmitted. It should be noted that the bandwidth of the transmitted and the reflected light is dependent on the Bragg grating characteristics, its length as well as the modulation depth [56].

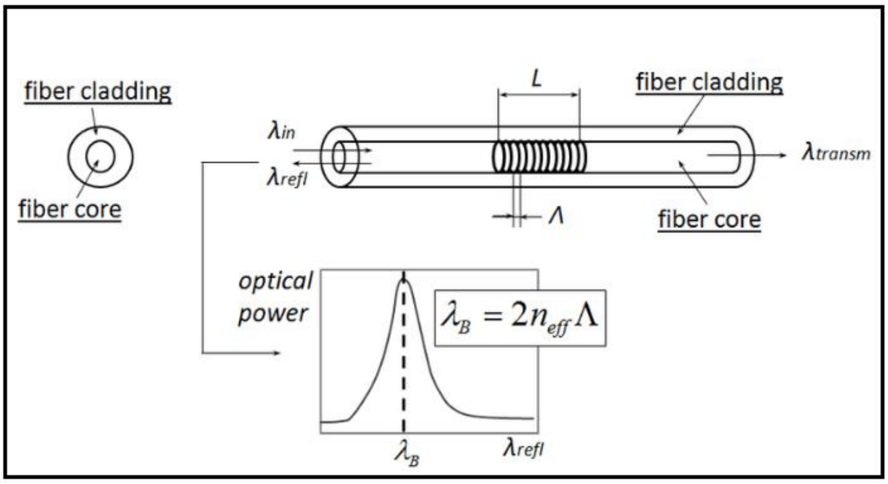

Figure 2.12 Schematic representation of a Bragg grating inscribed into the core of an optical fiber[56].

FBG has greatly improved the optical fiber components in that there is now:

1. Low losses
2. Done into the fiber
3. Easy shaping of the spectral response
4. Stability
5. Reduced maintenance

The compensating fiber component has a deal of grating with a variety of refractive indices that give various velocities for different modes of light signals to counterbalance for the delay between the two modes. The Bragg wavelength changes along the grating length whereby various frequency components of the incident beam are reflected

$$\boldsymbol{\lambda_B} = \mathbf{2}\,{}'n\Lambda \quad \textbf{(2.24)}$$

The grating dispersion Dg is

$$\boldsymbol{D_g} = \frac{\mathbf{2n}}{\boldsymbol{c}(\Delta\boldsymbol{\lambda})} \quad \textbf{(2.25)}$$

Where n is the average mode index, Δλ is the grating bandwidth, and c is the light velocity.

The compensation fiber has a higher negative dispersion as compared with DCF [20].

2.7.3 Dispersion Compensation with DCF

Upgrading the 1310 nm optimized optical fiber link to operate at 1550 nm is inducing a great interest. The higher value of the dispersion coefficient (D) at 1550 nm may be compensated by different compensation approaches. Among these, the DCF which has a relatively larger negative dispersion coefficient at 1550 nm is of a substantial importance practically. Compensating the dispersion effect in the fiber link, by a shorter DCF length, necessitates a relatively larger negative *D* value of the DCF. It has been illustrated that with a relatively larger difference in the refractive index (Δ), a high negative value of *D* can be achieved. Regrettably, with a higher value of Δ, the scattering loss will also increase, and this leads to applying an EDFA together with the DCF to compensate for dispersion [57].

2.8 Wavelength Division Multiplexing

They are three alternatives that are available to technically enhance an optical fiber communication system capacity. The first approach is referred to as space division multiplexing (SDM). This entails enhancing the deployed fiber links [58]. The second approach entails enhancing the bit rate per fiber with the use of time division multiplexing (TDM) [59]. The third approach entails enhancing the wavelengths number over the same fiber using WDM [60]. This thesis focuses on the third type of technology.

A WDM transmission link transmits larger amounts of data by multiplexing a spate of low capacity wavelength channels onto a single fiber. Using WDM thus allows for an increased capacity for long haul optical transmission systems. In general, a standard WDM system has three main parts:

(i) Transmitter section.
(ii) Transmission link section.
(iii) Receiver section [61].

The ranges of the aforementioned transmission systems may be classified as:

1. Long-haul optical fiber networks ranging from 600 to 1000 km.
2. Extended long-haul (ELH) ranging from 1000 to 2000 km.
3. Ultra-long-haul (ULH) ranging from 2000 to 4000 km [23].

2.8.1 WDM System Performance Parameters

The measurement of speed, independence of the digital structure of the signal and a wider range of the transmitted speeds predispose the quality factor (Q-factor) to monitor DWDM systems [62]. When planning an optical communications system, the bit error rate (BER) is a key parameter of the system design and performance indicator. The BER is always determined by the speed of the link, its power, the length (distance), and the prevalent noise [22]. Q-factor and BER are the most significant factors that constrain the transmission link in most optical communication systems. To transmit signals over longer distances, it is paramount to have the BER as low as possible and a high Q-factor. Q factor gauges the quality of an analogue transmitted signal with respect to its signal-to noise ratio (SNR). In that regard, it considers physical impairments to the signal like noise, chromatic dispersion and other non-linear effects that may degrade the signal and consequently lead to bit errors. Therefore, the higher the Q factor value the better the SNR and thus the lower the bit errors. The Q-factor in dB as a function of the number of spans N is depicted as:

$$\boldsymbol{Q_{dB}\ (N) = 20.\log\left[\frac{2.\frac{P_a.R_d}{DC}.\frac{R-1}{R}}{\sqrt{2NR_d^2(FG-1).hv.\frac{2P_a}{DC}B_e+\left(\frac{R_{sens}}{7}\right)^2+\sqrt{\left(\frac{R_{sens}}{7}\right)^2}}}\right]} \tag{2.26}$$

where Pa is the power difference in 1s and 0s; Rd is the responsivity of the photodiode; DC is the signal duty cycle for an NRZ signal, and in this case the duty cycle is unity; R is the extinction ratio; F is the noise figure for the amplifier; G is the amplifier gain; *hv* is the photon energy; and R_{sens} is the sensitivity of the receiver, and it is directly proportional to the PIN diode thermal noise [20]. In telecommunication, the BER is the percentage of bits with errors relative to the total number of bits that have been received in a particular transmission. As an example, a transmission link may have a BER of 10^{-6}, this means that 1 bit out of 1,000,000 bits transmitted, was in error. When the signal is strong and its path is unperturbed, this number as very small and tends to be insignificant. It however becomes significant if we want to maintain a better signal-to-noise ratio with the presence of imperfections in the transmission link brought about by the electronic circuitry (amplifiers, filters, and digital/analog converters and the propagation medium (e.g. optical fiber)) [63].BER may also be depicted in terms of the probability of error (POE),

$$\boldsymbol{POE} = \frac{1}{2}\left(\mathbf{1} - \mathbf{erf}\sqrt{\boldsymbol{E_b}/\boldsymbol{N_0}}\right) \qquad \mathbf{(2.27)}$$

Where *erf* is the error function, *Eb* is the energy in one bit and *No* is the noise power spectral density which is the noise power in a 1 Hz bandwidth.

The error function varies for each of the different modulation schemes. It is needful to note that probability of error (POE) is proportional to E_b/N_o, and that is a form of signal-to-noise ratio. The energy per bit, E_b, is determined by dividing the carrier power by the bit rate and it has unit of joules. Since *No* is in power (joules per second) per Hz (seconds), Eb/No is a dimensionless term, or just a numerical ratio [63].

2.8.2 WDM Techniques

There are many various technics that use special components that are being used to combine multiple wavelengths onto one fiber and separate them at the input of the receiver. Each of these technics has particular advantages and disadvantages. These can include thin-film filters, Bragg fiber gratings and arrayed waveguide gratings [64].

2.9 Thin Film Filter Technique

The thin-film filter can allow for only a narrow part of the spectral width to go through it and tends to reflect the other light that is outside this band. To make a wavelength multiplexing device to combine and/or separate N wavelength channels, $N-1$ thin-film filters need to be cascaded. Figure 2.13 shows a multiplexing function for four wavelengths λ1, λ2, λ3, and λ4.

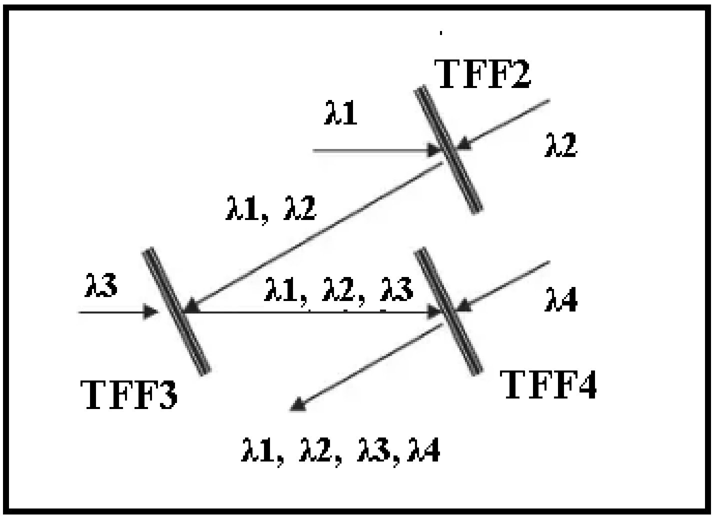

Figure 2.13 Illustration of multiplexing four wavelengths using thin-film filters [64].

As illustrated above, filters labeled TFF2, TFF3, and TFF4 allow wavelengths λ2, λ3, and λ4, respectively to pass through and reflect the others. These filters are anchored slightly at a given angle to guide light from one TFF to another. The first filter (TFF2) reflects λ1 and allows λ2 to go through. Then these two signals are reflected from the second filter TFF3 and this is where λ3 is coupled to them. After going through the same process at the third filter TFF4, the four wavelengths are coupled to the fiber by a lens mechanism. In order to decouple all the four wavelengths λ1, λ2, λ3, and λ4, the directions of the arrows are reversed. Since the filters are not ideally perfect and the light beam loses part of its power, this multiplexing scheme becomes effective for limited channels which are normally 16 or less [64] .

2.10 Fiber Bragg Grating Technique

The FBG allows for optical channels spacing which is as narrow as 25 GHz. Different from a thin-film filter, an FBG can reflect a narrower spectral part and allow for all the other wavelengths to go through. To make a device to combine or separate N wavelengths, $N-1$ FBGs and $N-1$ circulators need to be cascaded. Figure 2.14 shows a multiplexing function for four wavelengths λ1, λ2, λ3, and λ4 when using three FBGs and three circulators C2, C3, and C4. The fiber grating filters are labeled FBG2, FBG3, and FBG4 and are built to reflect wavelengths λ2, λ3, and λ4, respectively while passing all the others.

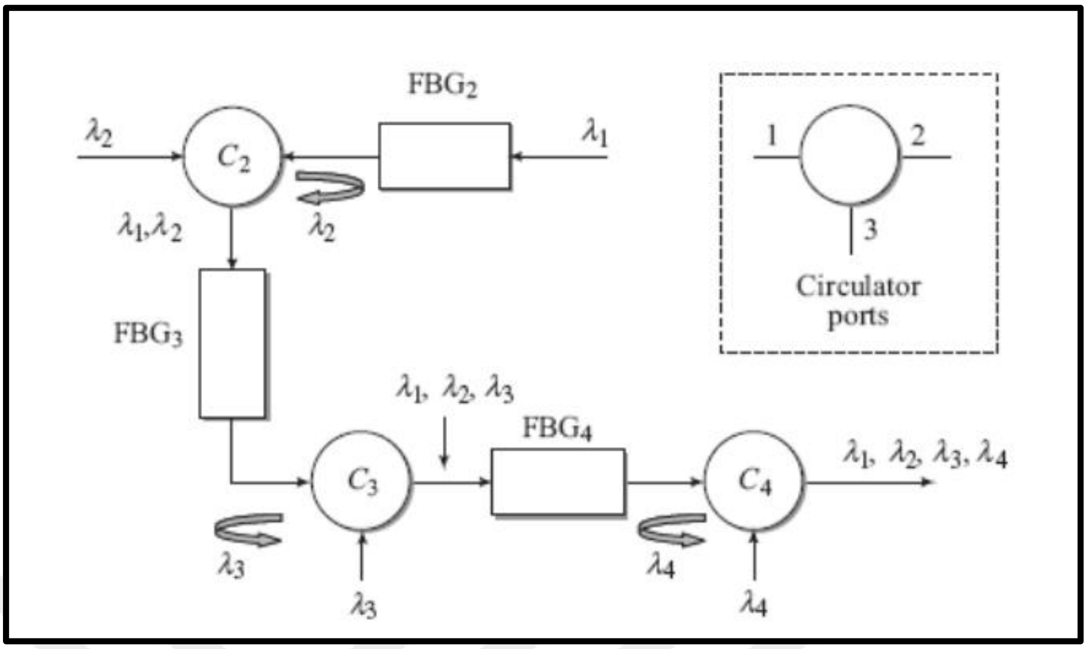

Figure 2.14 Multiplexing of four wavelengths using three FBG devices and three circulators[64].

In order to understand the operation of a multiplexer, consider combining a circulator C2 and a fiber filter FBG2. The filter FBG2 reflects wavelength λ2 and passes wavelength λ1. When λ1 gets through FBG2 it gets to port 2 of the circulator C2 and it exits from port 3. λ2 gets to port 1 of C2 and exits from port 2. After getting reflected from FBG2, it goes through port 2 of circulator C2 and exits from port 3 with λ1. Thereafter, at circulator C3, λ3 gets through port 3 of C3 and exits from port 1 and then goes to FBG3. After getting reflected from FBG3, it gets through port 1 of C3 and exits from port 2 with λ1 and λ2. After going through the same process at C4 and FBG4 to put in λ4, all the four wavelengths exit from port 2 of C4 and can easily be coupled into the fiber.

Like what happens when using thin-film filters to make multiplexers, the size constraint when employing fiber Bragg gratings is that just one filter is required for each of the wavelengths and in most cases the operation is successive with wavelengths being transmitted by a filter after the another. Hence, losses are not the same from one channel to the other, and this is because every wavelength passes through different circulators and fiber gratings, and all those add losses to the channel. This can be satisfactory if the number of channels is small, but the loss between the first and last wavelengths may be a constrain for many channels [64].

2.11 Arrayed Waveguide Gratings

AWG has input and output slab waveguide arrays, two similar focusing star couplers, and an inter-connection of waveguides that are not coupled known as the grating array. Within the grating array area, the length of the path of each of the waveguide varies by a somewhat accurate amount ΔL from the length of the adjacent arms. The difference in the path length brings about some spaced delays in the phase of the signal in each of the adjacent arms, thenceforth the array makes a Mach-Zehnder grating. Eventually, the second lens in region 5 focuses each of the wavelengths onto another exit port in the output slab array in region 6. Conversely, if N wavelengths are put in N separate fibers (from right to left in Figure 2.15 (a,b)), they all get out at the same port on the left. These devices are commonly used because they have good features such as 25-GHz (0.4-nm at 1550 nm) channel spacing and the fact they are somewhat compact and can be fabricated on silica wafers easily and as well made for a big number of WDM channels. Devices from 8 to 40 channels are commercially available [64].

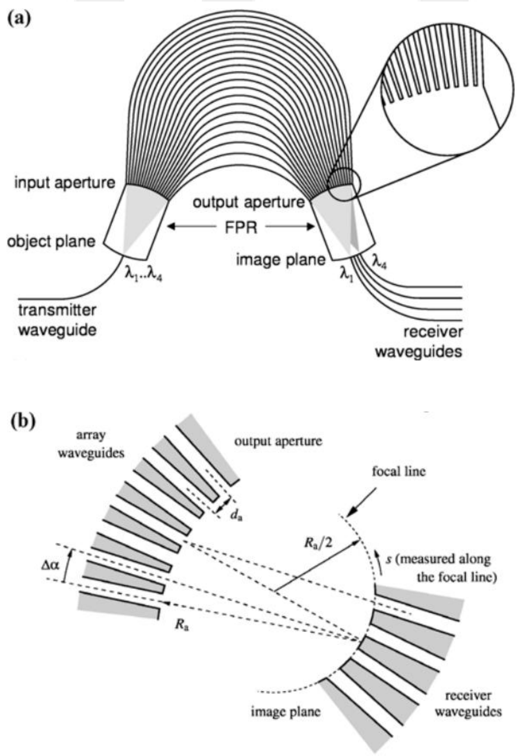

Figure 2.15 (a) Geometry of an AWG demultiplexer, (**b**) beam focusing geometry in the free propagation region

CHAPTER 3

METHODOLOGY

3.1 Introduction

This chapter shows the methodology adopted in this study work. The First section of this chapter illustrates the general procedures undertaken to accomplish the aim of this research. Beside includes definitions of the essential performance parameters for fiber amplifier, the components utilized in simulation design. Moreover, the investigation and optimization of hybrid fiber amplifier are discussed. Finally, it explains the effect of cascading amplification stages.

3.2 General Research Flowchart

The general research flowchart of this research work is shown in Figure 3.1. In this work, CSP Hybrid fiber amplifier configuration is simulated via OptiSystem-14, it is an innovative, powerful and rapidly evolving software design tool. It enables users to test, plan and simulate almost all types of optical link this work is divided into two essential parts: optimization and characterization. The optimization is divided into three categories, namely the pump wavelength, the pump power and the coupling ratio optimization. In the pump wavelength optimization, the wavelength of EDFA and RFA2 was set at 1480 nm while RFA1 is pumped 1410 nm and 1495 nm. The pump power optimization is determined at the broad gain bandwidth within 3-dB and higher average gain level that can be acquired, whereas for coupling ratio optimization, the coupling factor was changed from 0.2 to 0.8 with a step of 0.1.

3.3 The Design Parameters of a Fiber Amplifier

The main design metrics of the aforementioned amplifiers are the wavelength and power of the incoming signal as well as the pump power. The following is their elucidation.

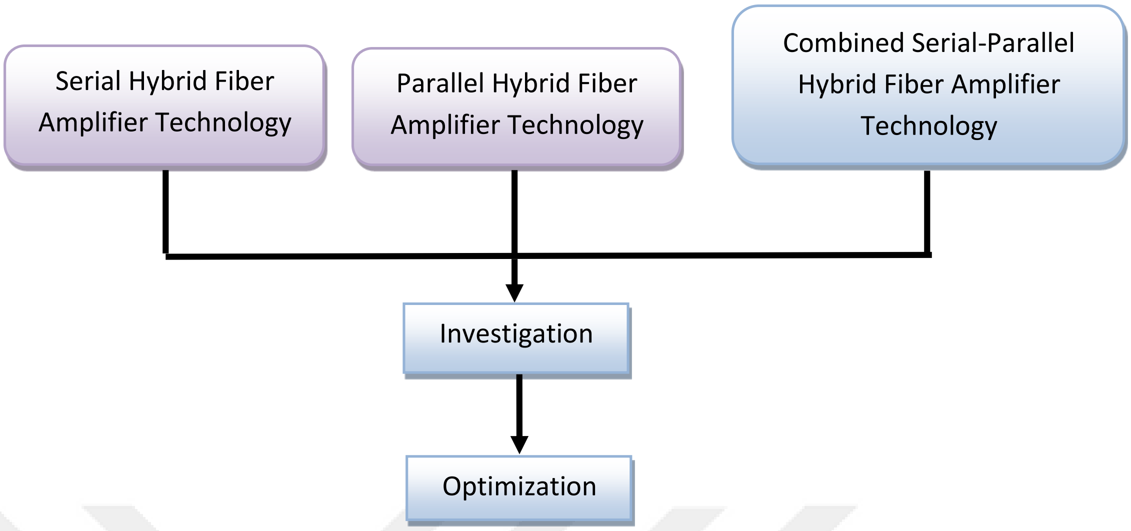

Figure 3.1 General research process flow chart

3.3.1 The Wavelength of the Input Signal

To ascertain the gain bandwidth, the wavelength of the input signal is swept between 1510 nm and 1630 nm inside a 150 kHz linewidth.

3.3.2 The Power of the Input Signal

The power of the input signal for the aforementioned amplifiers is got from a laser source that is tunable with its power ranging from –30 dBm to -6 dBm having 2 dBm step for gain dynamic range and spectra monitoring.

3.3.3 The Pump Power

There are two pump unit which are RPU1 with a maximum power of 850 mw and 600 mw for the first and second order pumping, respectively the other pump is RPU2 that used for pumping EDF1 and RFA2 with 15.6 mw, 600 mw respectively. In combined serial parallel hybrid fiber Amplifier technology, the pump wavelength is tuned at 1480 nm for both EDF and RFA2 whereas the pump wavelength of RFA1 is 1410 nm with 1495 nm.

3.4 The Performance Parameters of a Hybrid Fiber Amplifier

The performance parameters of an amplifier are regarded to be the efficiency determinant of that particular system and are used to determine the quality of other technics used. When an HFA is considered to depend on a somewhat composite share between the two medium of gain, the effective performance parameters may be set with the optimization of the share.

In the succeeding sections, some of these most parameters that are more important are explained.

3.4.1 The Gain of the Amplifier

The signal/amplifier gain may be regarded as the most significant parameter for an optical amplifier [65].

$$\boldsymbol{G = \frac{P_{out}}{P_{in}}} \quad \textbf{(3.1)}$$

Where; G is the amplifier gain, P_{in} and P_{out} are the input and output signal powers, respectively.

Nonetheless, there are other parameters that are related to amplifier gain that are used to assess the gain performance. These include; gain bandwidth, average gain, gain saturation and gain variation. Below is an explanation of these parameters.

3.4.1.1 The Average Gain

The gain of an amplifier may be depicted in terms of the average gain in a peculiar bandwidth (λ_1 to λ_n) wherein the average gain is the sum total of all the values of the gain divided by the wavelengths number [13].

$$\boldsymbol{G_{av} = \frac{G(\lambda_1)+G(\lambda_2)+ \; ....+G(\lambda_n)}{n}} \quad \textbf{(3.2)}$$

Where: G_{av} is the amplifier average gain, G (λ_1) is the gain at peculiar wavelengths λ_1, and n is the wavelengths number of in the whole bandwidth.

3.4.1.2 The Gain Variation

This describes the gain flatness within a particular bandwidth is the gain variation and can be depicted as:

$$\boldsymbol{G_{var} = G_{max} - G_{min}} \tag{3.3}$$

Where: G_{var} is the gain variation, G_{max} is the maximum gain and G_{min} is the minimum gain.

3.4.1.3 The Bandwidth of the Gain

This is sometimes called the amplification bandwidth. It is the optical wavelength range where gain is highest. Additionally, the gain bandwidth may be taken to be the full-width at half-maximum (FWHM) for the logarithmic gain, and it is gauged in decibels, the Figure 3.2 shows the gain parameters which used to evaluate the amplifier gain [66].

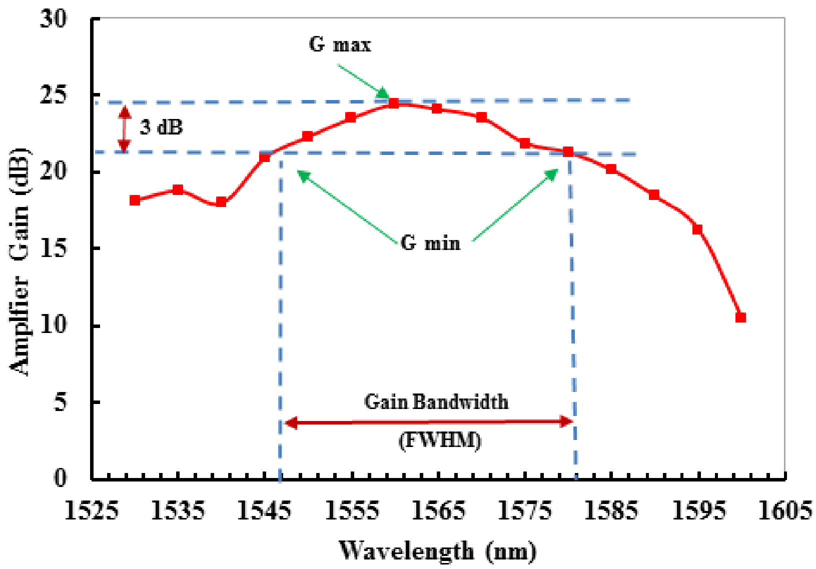

Figure 3.2 Gain parameters used to evaluate the amplifier gain [66].

3.4.1.4 Gain Saturation

In optical amplifiers, the gain is constant for small power values of the signal, and when the input signal-power goes beyond a particular value, the gain deteriorates. This power level is known as the saturation power ($P_{sat.}$) and the phenomenon is called "gain saturation" and it appears when the power of the signal increases. At this instance the amplifier saturates and doesn't give out any additional output power, thus a decrease in the gain, the amplifier gain saturation is shown in Figure 3.3.

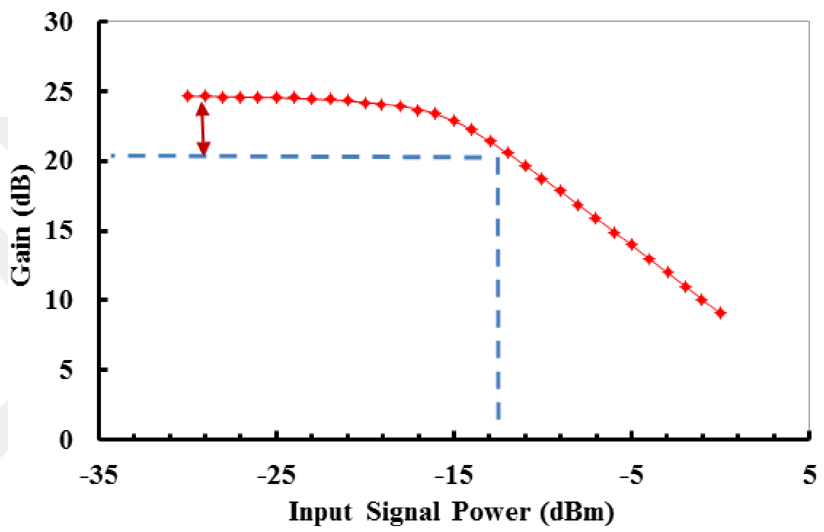

Figure 3.3 Amplifier gain saturation [66].

3.4.2 Noise Figure

The noise figure (NF) is used to measure the noise added to the signal due to the prevalence of an amplifier. Prior to the light getting into an amplifier, the ingress signal-to-noise ratio is known as SNR_{in}, and the one after is SNR_{out}. Hence, the NF may be taken to be the ratio of SNR_{in} to SNR_{out}. Therefore, the NF depicts the fall in the signal-to-noise ratio of an optical amplifier.

3.5 Simulation Software Components

The components and equipment that used in the simulation analysis is recorded in Table 3.1.

Table 3.1 General specifications of the components used in simulation analysis.

Components	**General Specifications**
Tunable Laser Sources (TLS)	Wavelength: 1510 nm-1630 nm Linewidth: 150 kHz Power: (–30 dBm - 6 dBm)
EDF	Length: 3 m Core radius and Er doping radius:1.65 µm
EPU	Operating wavelength: 1480 nm Power: 15.6 mW
DCF	Length: 7 Km Effective area: 20 µm^2 Dispersion: –110 ps/nm/km
RPU1	Operating wavelength: 1410 nm, 1495 nm. Power: 850 mw, 650 mw
RPU2	1480 nm, 600 mw
OSA	Resolution bandwidth: 0.01 nm Wavelength range: 1495-1630 nm
WDM/WSC	Wavelength: 1480 nm / C+L-band Wavelength: 1495 nm / L-band
VOC	Optimum ratio = 0.4,0.8 for -15 dBm, -30 dBm
WDM Transmitter	Modulation type: RZ Bit rate: 40 Gbps Freq. Spacing: 250 GHZ
SMF	Length:44 km

CHAPTER 4

RESULTS AND DISCUSSION

4.1 Introduction

The suggested design of Combined Serial Parallel Hybrid Fiber Amplifier (CSP-HFA) has two parts, the first part is about cascading (connecting) two stages of amplification for a linear EDFA and a nonlinear RFA1, the other part is RFA2 (nonlinear) which is parallel with the first part. In CSP-HFA architecture the input is divided into two parts depending on the value of the coupling ratio. Although this kind of amplifier has got somewhat higher gain and good NF, the conversion efficiency of the pump in the RFA stage is deficient. In this chapter, the EPP, RPP1, and RPP2 are optimized wherein high average gains with low gain variations are achieved.

4.2 Simulation Design

Figure 4.1 shows the proposed setup of a serial parallel HFA. The setup consists of serial RFA1/EDFA in the first branch and RFA2 in the second branch. The input signal power was controlled and divided into two input power ratios via variable optical coupler (VOC). The input signal power was varied from 1530 nm to 1630 in the step of 5 nm with an input power range of -30 dBm to -15 dBm. RFA1 was pumped by two RPUs of 1510 (800 mw) and 1495 nm (650 mw). High RPU of 1410 was used in order to achieve both first and second order stimulated Raman scattering (SRS) that have Raman peak gain at 1510nm and 1610nm respectively. The first order SRS signal can achieve gain in S-band region. On the other side, an ultra L-band gain can be achieved by the second order SRS signal which boost the L-band gain provided by RFA2. While RFA2 was pumped by 1480 nm pump power. In addition, EDFA was pumped by the residual pump power from RFA2 via wave selective coupler (WSC). The input signal at first is divided into two parts via VOC to be inserted into these two amplifier stages. The ratio of the input signal was varied from 10:90 to 90:10 for each input signal power value so the optimal result can be achieved; the simulation setup is shown in Figure 4.2.

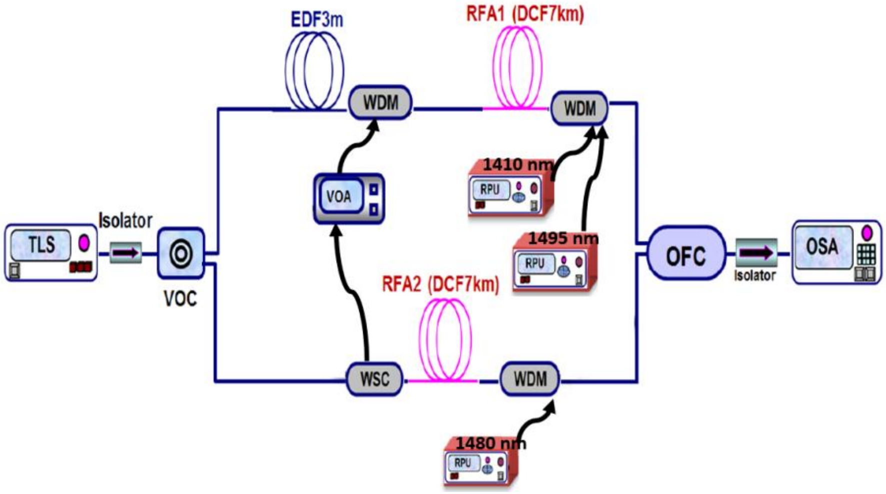

Figure 4.1 The proposed serial parallel HFA.

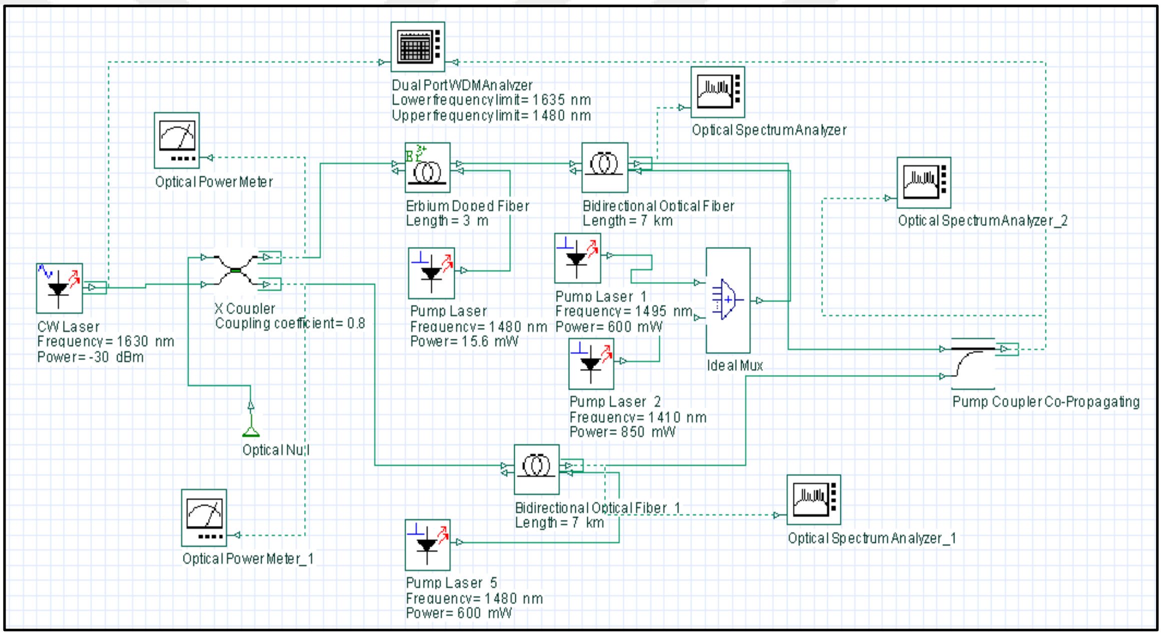

Figure 4.2 Simulation setup

4.3 First and Second Order Stimulated Raman Scattering

In the first step, the appearance of first order stimulated Raman scattering (SRS1) was investigated as a function of RP1 power rangers (0-800 mw) as illustrated in Figure 4.3. It can be noticed that SRS1 with a wavelength of 1512 nm starts to oscillate at RP1 of 400 mw. Further increment in the pump power until 600 mw, SRS1 becomes more effective. Then it was saturated at pump power value of 800 mw. The wavelength of the generated SRS1 could achieve good flatness gain in the S-band region.

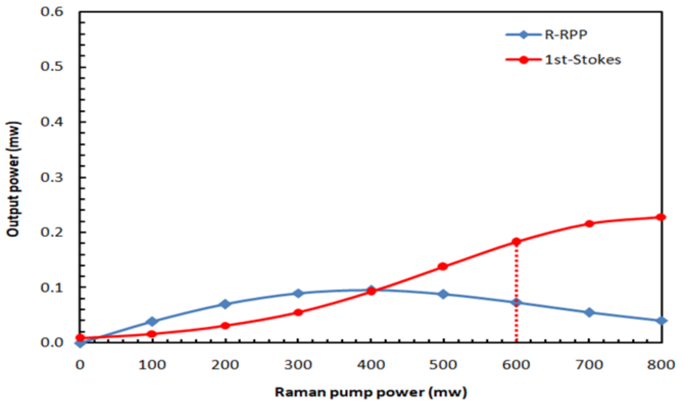

Figure 4.3 First order stimulated Raman scattering (SRS1).

In this context, high order stimulated Raman scattering (SRS2) that has wavelength of 1612 nm (200 nm away from the pump wavelength) is needed to boost the overall gain of the optical amplifier within ultra-long band (ultra L-band). Refereeing to Figure 4.3, SRS1 was saturated at 800mW. Therefore, in order to achieve higher order SRS signal, RP1 power was extended in rang from (0-2000 mw) as illustrated in Figure 4.4. It is clear from the results that SRS2 was starts to be effective at RP1 of 900 mw. By increasing the pump power further, SRS2 was saturated at pump power of 1300 mw. At this point SRS3 was which has a wavelength of 1712nm (300 nm away from pump power wavelength of 1412). The generated SRS3 will not be used as its far from infrared band of the optical fiber.

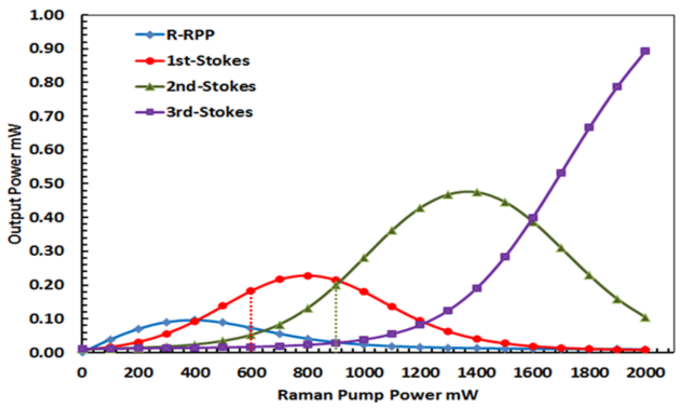

Figure 4.4 Second order stimulated Raman scattering (SRS1).

4.4 Raman Pump Power Optimization

The overall HFA gain was optimized in terms of RP1 power as indicated in Figure 4.5. The input signal ratio was 50:50. It can be noticed that different overall gain flatness was achieved for different pump powers. Starts with 500 mw, an overall gain flatness of 40 nm with an acceptable average gain of 17 dB was presented. The gain average was improved to 18.1 dB while the same gain flatness was produced using 600 mw pump power. Both of flatness gain and the average power were improved by increased the pump power to 700 mw. A result obtained were 80 nm and 18.6 dB for gain flatness and average gain respectively. Same behavior was recorded with the increment of the pump power until it reached saturation at pump power of 900 mw. At this point a maximum gain flatness of 95 nm and the highest average gain of 19.8 dB were observed.

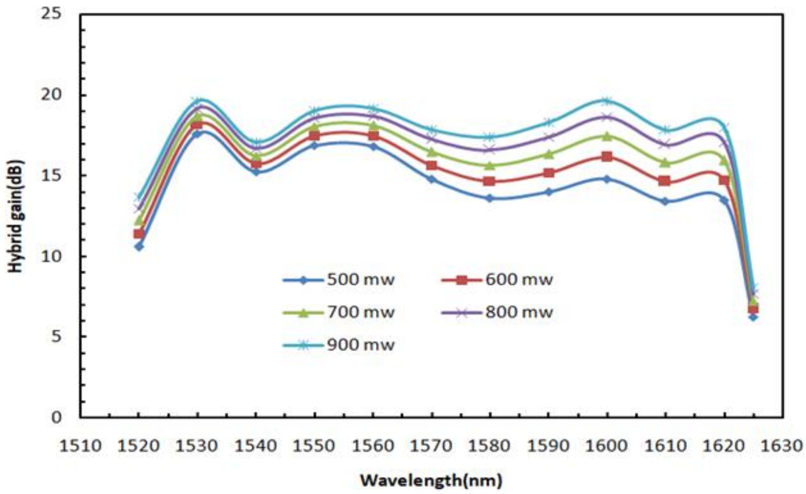

Figure 4.5 Overall gain of HFA vs. RP1 power.

4.5 Overall Gain Specturm Under Difffernt Input Signal Ratio

The proposed serial parallel HFA was firstly examined under two input signal powers of -25 dBm and -15 dBm. These two-input signal powers were chosen in order to show both of non-saturation and saturation behavior of the proposed amplifier setup. Figure 4.6(a, b) shows the overall gain saturation at these two-input signal respectively. In this figure the input signal ratio that inserted to each branch was controlled by the VOC so when n is inserted to one branch (EDFA and RFA1), (1-n) will inserted to other branch (RFA2). It is clear from Figure 4.6.a that when n was increased the overall gain was increased too. Same behavior was recorded and there was no saturation took place at such low input power. On the side, Figure 4.6.b shows the overall gain spectrum at -15 dBm under the same input signal power ratios. It is clear that when n was increased, the overall gain suffers from saturation especially in ultra L-band region.

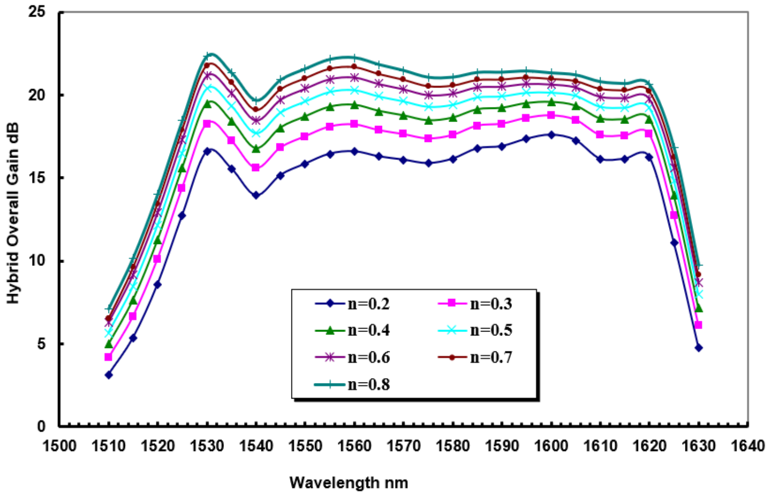

(a)

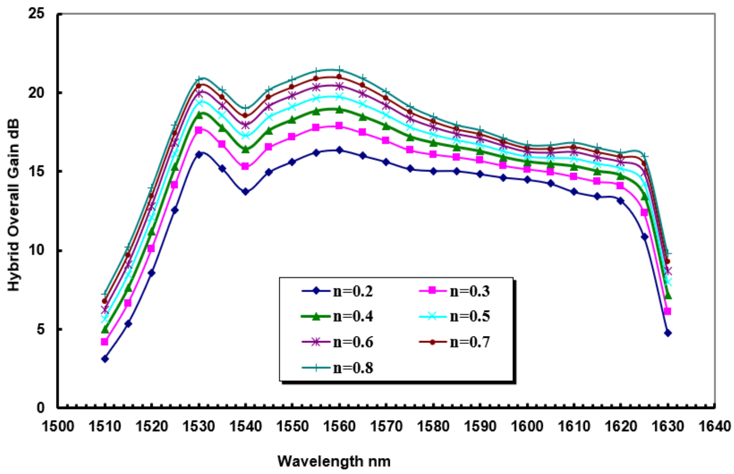

(b)

Figure 4.6 Overall gain spectrum of the serial parallel HFA versus different signal power (a) -30 dBm and (b) -15 dBm.

It is very important to find the optimum flatness gain of the overall gain spectrum at these two different input signals power. In this context, the optimal input signal ratio for small signal input power of -30 dBm was (n=0.8). At this input ratio the overall gain flatness bandwidth recorded was 95 nm (1525 nm-1620 nm) that covers all of S+C+L bands. In addition, a high average gain level of 20 dB and an acceptable noise figure of 5.9 dB were achieved as depicted in Figure 4.7.a. The gain flatness bandwidth was reduced under -15 dBm input power under the all input signal ratio conditions. The highest gain flatness recorded was at the input signal power ratio of (n=0.4). Up to 85 nm (1530 nm-1615 nm) with a gain average power of 17 dB and a highest noise figure of 9 dB were observed as depicted in Figure 4.7.b.

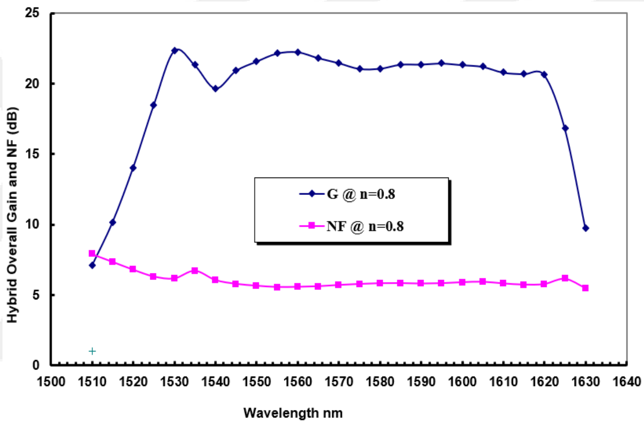

(a)

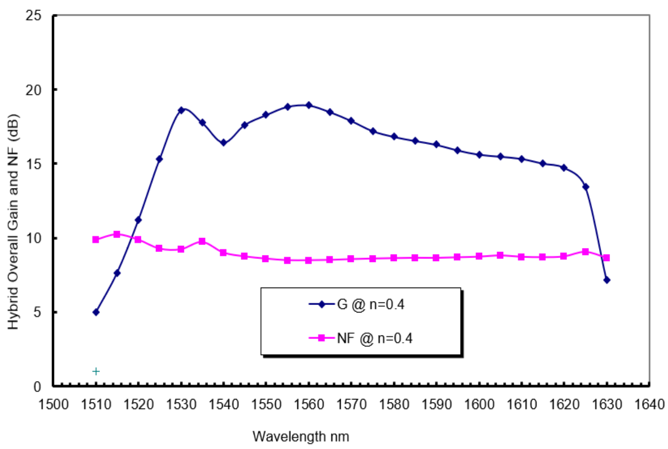

(b)

Figure 4.7 Optimal Gain spectrum and noise figure of the serial parallel HFA versus different signal powers; (a) -30 dBm and (b) -15 dBm

Figure 4.8 illustrates the overall gain as a function of the input signal power at two different amplification regions of C-band (1530 nm) and L-band (1595 nm). It can be seen that the overall gain at C-band region exhibited wider input dynamic range comparing to the input dynamic range achieved in L-and region. The input dynamic range is defined as the input signal power range at which the overall gain is not saturated yet. In the other word, the overall gain was saturated faster at 1595 nm. This behavior can be easily understood by looking carefully to the Figure 4.8 at which the overall gain was saturated at -15 dBm.

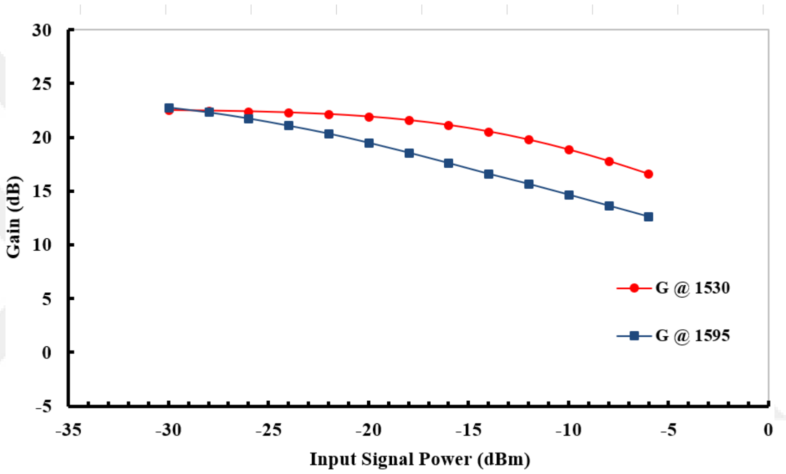

Figure 4.8 Gain level versus input signal power at two different wavelengths1530 nm and 1595 nm

CHAPTER 5

CONCLUSION

A serial parallel HFA that combine both an EDFA an RFA1 in one branch and RFA2 at the other branch has been simulated using Optisystem 14. In the proposed setup, the overall gain spectrum was tested under two different input signal power of -25 dBm and -15 dBm. The VOC was incorporated to control the input signal power ratios inserted to each of the amplifier branches. It can be clearly seen that this ratio plays an important rule to the overall gain flatness optimization. Two different input ratios were recorded that gives an optimal gain bandwidth which highly depending on the overall gain saturation region. In another word, low input signal power ratio was needed when the amplifier starts to saturate. Moreover, the first and second order Raman scattering can be achieved by using high pump power for RP1. The first order stimulated Raman scattering can support S band region whereas the second order stimulated Raman scattering can be used as a booster amplification band for L band region which assist the amplification band caused by the RP2 unit. On the other side, good flatness gain in C-band region can be achieved by EDFA. The proposed design of CSP-HFA produced broadly gain flatness bandwidth of 95 nm (1525 nm-1620 nm) with an average gain of 19 dB and relatively low noise figure of 5.9 dB at low input signal power of -25 dBm.

REFERENCES

[1] Carena, A., Curri V., & Poggiolini, P. On the Optimization of Hybrid Raman / Erbium-Doped Fiber Amplifiers. IEEE Photonics Technol. Lett. *13*(11) 1170-1172. 2001.

[2] Ali, M. H., Abdullah, F.,Jamaludin, M. Z., Al-Mansoori, M. H., Al-Mashhadani, T. F., & Abass, A. K. Simulation and experimental validation of gain-control parallel hybrid fiber amplifier. J. Opt. Soc. Korea, *18* (6) 657-662. 2014.

[3] Ma,M. X.,Kidorf, H.D., Rottwitt, K., Kerfoot, F. W., & Davidson, C. R. 240-km repeater spacing in a 5280-km WDM system experiment using 8 × 2.5 Gb/s NRZ transmission. IEEE Photonics Technol. Lett. *10*(6) 893-895. 1998.

[4] Baney, D. M., & Stimple, J. WDM EDFA gain characterization with a reduced set of saturating channels. IEEE Photonics Technol. Lett., *8*(12) 1615-1617. 1996.

[5] Wysocki, P. F., Judkins, J. B., Espindola, R. P.,Andrejco, J. P., & Vengsarkar, A. M. Broad-Band Erbium-Doped Fiber Amplifier Flattened Beyond 40 nm Using Long-Period Grating Filter, *9*(10) 1343-1345. 1997.

[6] Masuda, H., & Kawai, S. Wide-band and gain-flattened hybrid fiber amplifier consisting of an EDFA and a multiwavelength pumped Raman amplifier. IEEE Photonics Technol. Lett., *11* (6) 647-649. 1999.

[7] Lee, J. H., Chang, Y. M., Han, Y. G., Kim, S. H., Chung, H., & Lee, S. B. Dispersion-compensating Raman/EDFA hybrid amplifier recycling residual Raman pump for efficiency enhancement. IEEE Photonics Technol. Lett., *17*(1) 43-45. 2005.

[8] Masuda, H., Kawai, S., Suzuki, K.-I., & Aida, K. Ultrawide 75-nm 3-dB gain-band optical amplification with erbium-doped fluoride fiber amplifiers and distributed Raman amplifiers. IEEE Photonics Technol. Lett., *10* (4) 516-518. 1998.

[9] Kawai, S., Masuda, H., Suzuki, K. I., & Aida, K.Wide-bandwidth and long-distance WDM transmission using highly gain-flattened hybrid amplifier. IEEE Photonics Technol. Lett., *11*(7) 886-888. 1999.

[10] Min, B., Yoon, H., Lee,W. J., & Park, N. Coupled Structure for Wide-Band EDFA with Gain and Noise Figure Improvements from C to L-Band ASE Injection. IEEE Photonics Technol. Lett., *12* (5) 480-482. 2000.

[11] Pizzinat, A., Santagiustina, M., & Schivo, C. Impact of hybrid EDFA-distributed Raman amplification on a 4 × 40-Gb/s WDM optical communication system. IEEE Photonics Technol. Lett., *15*(2) 341-343. 2003.

[12] Yeh, C. H., Lee, C. C., & Chi, S. 120-Nm Bandwidth Erbium-Doped Fiber Amplifier in Parallel Configuration. IEEE Photonics Technol. Lett., *16* (7) 1637-1639. 2004.

[13] Liaw , S. K., Huang, C. K., & Hsiao , Y. L. Parallel-type C+L band hybrid amplifier pumped by 1480 nm laser diodes. Laser Phys. Lett., *5*(7) 543-546. 2008.

[14] Guo , M. N., Liaw, S.-K., Shum, P. P., Chen, N.K., Hung , H.-K., & Lin, C. Single-wavelength-pump bi-directional hybrid fiber amplifier for bi-directional local area network application. Opt. Commun., *284*(2) 573-578. 2011.

[15] Singh, S., & Kaler, R. S. Flat-gain L-band raman-EDFA hybrid optical amplifier for dense wavelength division multiplexed system. IEEE Photonics Technol. Lett., *25* (3) 250-252. 2013.

[16] Singh, H., & Singh, S. Performance Analysis of Hybrid Optical Amplifiers in 120 x 10 Gbps WDM Optical Network with Channel Spacing of 50 GHz. 55-58. 2014.

[17] Ali, M. H., Abdullah, F., Jamaludin, M. Z., Al-Mansoori, M. H., Abass, A. K., & Al-Mashhadani, T. F. Effect of cascading amplification stages on the performance of serial hybrid fiber amplifier. Fiber Integr. Opt., *34*(3) 157-170. 2015.

[18] Sharma, S. R., & Sharma, V. R. Gain flattening of EDFA using hybrid EDFA/RFA with reduced channel spacing. 3rd Int. Conf. Signal Process. Integr. Networks , 260-264. 2016.

[19] Hassan, A. M., Aboshosha, A., & El Mashade, M. B. Analysis of Gain and NF using Raman and hybrid RFA-EDFA Analysis of Gain and NF using Raman and hybrid RFA-EDFA. J. Multidiscip. Eng. Sci. Technol., *4* (10) 8482-8487. 2017.

[20] Tahhan, S. R., Ali, M. H., & Abass, A. K. Characteristics of Dispersion Compensation for 32 Channels at 40 Gb/s under Different Techniques. J. Opt. Commun., 1-9. 2017.

[21] Kaur, I., & Gupta, N. Hybrid Fiber Amplifier. in Optical Communications Systems, D. N. Das, Ed. InTech, 103-122. 2012.

[22] Dutton H. J. R., "*Understanding Optical Communications*", USA: IBM International Technical Support Organization, 157-184. 1998.

[23] Senior J. M., Jamro M. Y., "*Optical Fiber Communications: Principles and Practice*", London: prentice hall financial times, 2009.

[24] Ghatak A. G., Thyagarajan K., "introduction to fiber optics." cambridge university press, new delhi, 1998.

[25] Kobtsev, S. M., & Pustovskikh, A. A. Improvement of Raman Amplifier Gain Flatness by Broadband Pumping Sources. Laser Phys., *14*(12) 1488-1491. 2004.

[26] Tiwari, S. K., Jaiswal, P. A. K., Kumar, M., & Singh, S. S. Performance Analysis of Optical Amplifiers for Incorporation in Optical Network. Int. J. Adv. Technol. Eng. Sci., *2*(10) 238-247. 2014.

[27] Shafeena, P. K., Thomas, H., Kumar, M., & Sindhu, N. An EDFA Based Optical Communication System Compensating the Effects of Jitter and Transients with Maximum Gain flattening. Int. J. Eng. Technol. Manag. Sci., *2* (4) 190-195. 2014.

[28] Becker, P. C., Olsson, N. A. & Simpson, J. R."*Erbium-Doped Fiber Amplifiers Fundamentals and Technology*", New York: Elsevier, 234–304, 1999.

[29] Iizuka, K., "*Erbium-doped fiber amplifier*". University of torronto, canada. April 2003.

[30] Cavaciuti, A. & Sordo, B. Noise Measurements in EDFAs. Conference on Optcial Fiber Communications (OFC), (163),WM9, 1994.

[31] Headley, C. & Agrawal, G. "*Raman Amplification in Fiber Optical Communication Systems*". USA: Elsevier Academic Press, 33–97, 2005.

[32] Dakin, J. P. & Brown, R. G. W. "*Handbook of Optoelectronics*" (two-volume set). USA: CRC Press, 533–565, 2006.

[33] Agrawal, G. P., "*Applications of Nonlinear Fiber Optics*", San Diego: Academic press, 2008.

[34] Agrawal, G. P., "*Nonlinear Fiber Optics*", 4th ed. USA: Academic press, 274-350, 2007.

[35] Shen, Y. R., "*The Principles of Nonlinear Optics*", John Wily and Sons, Inc, New York, 141-186, 1984.

[36] Stolen, R. H., Ippen, E. P., & Tynes, A. R. Raman oscillation in glass optical waveguide. Appl. Phys. Lett., *20*(2) 62-64. 1972.

[37] Shuker, R., & Gammon, R. W. Raman-scattering selection-rule breaking and the density of states in amorphous materials. Phys. Rev. Lett., *25* (4) 222-225. 1970.

[38] Chraplyvy, A. R. Optical Power Limits in Multi-Channel Wavelength-Division Multiplexed Systems due to Stimulated Raman Scattering. Electron. Lett., *20*(2) 58-59. 1984.

[39] Ferreira, M. F., Rocha, J. F., & Pinto, J. L. Impact of Stimulated Brillouin Scattering on Fiber Raman Amplifiers. Electron. Lett., *27*(17) 2-3. 1991.

[40] Kobyakov, A., Mehendale, M.,Vasilyev, M., Tsuda, S., & Evans,A.F. Stimulated Brillouin scattering in Raman-pumped fibers: A theoretical approach. J. Light. Technol., *20* (8) 1635-1643. 2002.

[41] Fernando, M. Impact of Stimulated Brillouin Scattering in Optical Fibers with Distributed Gain. J. Light. Technol., *13* (8) 1692-1697. 1995.

[42] Chen, W., Wang, K., & Meng, Z. Stimulated Brillouin scattering effect on gain saturation of distributed fiber Raman amplifiers. Chinese Opt. Lett., *8* (4) 365-367. 2010.

[43] Farahani, M. A., & Gogolla, T. Spontaneous Raman scattering in optical fibers with modulated probe\nlight for distributed temperature Raman remote sensing. J. Light. Technol., *17* (8) 1379-1391. 1999.

[44] Wan, P., & Conradi, J. Impact of Single and Double Rayleigh Backscattering on Available System Gain in Optically Amplified Fiber Systems without Isolators. Candian Conf. Electr. Comput. Eng., 237-240. 1996.

[45] Hansen, P. B., Eskildsen, L., Stentz, A. J., Strasser, T. A., Judkins, J., DeMarco, J. J., Pedrazzani, R., & DiGiovanni, D. J.Rayleigh scattering limitations in distributed Raman pre-amplifiers. IEEE Photonics Technol. Lett., *10* (1) 159-161. 1998.

[46] Kamiya, T., Krausz, F., Monemar, B., Venghaus, H., Weber, H., Weinfurter, H., Raman amplifiers for telecommunications 1. New York: Springer, 2003.

[47] Iizuka, K. “*Elements of Photonics*”, (2), New York: Wiley and Sons,INC., 2002.

[48] Agrawal, G. P.,“*Fiber-Optic Communications Systems*”, Third Edition., (6), New York: Wiley-interscience, 2002.

[49] Karásek, M., Menif, M., & Rusch, L. A. Output power excursions in a cascade of EDFAs fed by multichannel burst-mode packet traffic: Experimentation and modeling. J. Light. Technol., *19* (7) 933-940. 2001.

[50] Bahrampour, A. R., Farman, F., & Ghasempour, A. The moment method for fiber Raman amplifier gain ripple minimization. Opt. Commun., *281* (14) 3673-3680. 2008.

[51] Hwang, S., Song, K.-W., Song, K.-U., Park, S.-H., Nilsson, J., & Cho, K. Comparitve high power conversion efficency of C-plus L-band EDFA. Electron. Lett., *37* (25) 1539-1541. 2001.

[52] Sakamoto, T., Aozasa, S. I., Yamada, M., & Shimizu, M. Hybrid fiber amplifiers consisting of cascaded TDFA and EDFA for WDM signals. J. Light. Technol., *24* (6) 2287-2295. 2006.

[53] Lee, J. H., Chang, Y. M., Han, Y. G., Chung H., Kim, S. H., & Lee, S. B.. A detailed experimental study on single-pump Raman/EDFA hybrid amplifiers: Static, dynamic, and system performance comparison. J. Light. Technol., *23*(11) 3484-3493. 2005.

[54] Oliveira, J. R. F., Moura, U. C., & Oliveira, J. C. R. F. Hybrid Distributed Raman / EDFA Amplifier with Hybrid Automatic Gain Control for Reconfigurable WDM Optical Networks. J. Microwaves, Optoelectron. Electromagn. Appl., *12* (2) 192-206. 2013.

[55] JR Elijah Kannatey-Asibu, “*Principles of Laser Materials Processing*”. canada: A John wiley & sons, 2009.

[56] Series, S., Sciences, O., Wavelength Filters in Fibre Optics,(123), September. Springer, 2006.

[57] Thyagarajan, K., Varshney, R. K., Palai, P., Ghatak, A. K., & Goyal, I. C. A novel design of a dispersion compensating fiber. IEEE Photonics Technol. Lett., *8*(11) 1510-1512. 1996.

[58] Essiambre, R. J., Ryf, R., Fontaine, N. K., & Randel, S. Breakthroughs in photonics 2012: Space-division multiplexing in multimode and multicore fibers for high-capacity optical communication. IEEE Photonics J., *5*(2). 2013.

[59] Huang, J. & Yao, J. Performance comparison between 160Gb/s WDM and TDM systems. Opt. - Int. J. Light Electron Opt., *123*(24) 2254-2259. 2012.

[60] Keiser, G. E., A Review of WDM Technology and Applications. Opt. Fiber Technol., *5*(1) 3-39. 1999.

[61] singh, S., sharma, M. Investigating the Q-factor and BER of a WDM system in Optical Fibre Communication using different modulation formats at different wavelengths. Int. J. Innov. Sci. Res., *4* (12) . 2015.

[62] Ivaniga,T., Ivaniga, P.Evaluation of the bit error rate and Q-factor in optical networks. IOSR J. Electron. Commun. Eng., *9* (5) 01-04. 2014.

[63] Breed, G., Bit Error Rate : Fundamental Concepts and Measurement Issues. High Freq. Electron.,January, 46-48. 2003.

[64] Keiser, G., "*Optical fiber communications*", 3rd ed. McGraw-Hill, 423–454, 2003.

[65] Keiser, G., "*Optical fiber communication*", MGH International Editions, Singapore. 670, 2014.

[66] Siegman, A. E., "*Lasers*", (37). USA: University Science Books, 264-297, 1986.

CURRICULUM VITAE

PERSONAL INFORMATION

Name Surname : Ayman ABOUSEDA

Date of Birth : 18.11.1987

Phone : 05436153137

E-mail : aymanabosida@yahoo.com

EDUCATION

High School : AL-ZOBIER BEN AL-AWAM

Bachelor : Tripoli University

Master Degree : Ankara Yildirım Beyazit University

TOPICS OF INTEREST

- Optical communication system
- Electronic circuits
- Antenna